Living in a Ghost Town:

The Geography of Depopulation and Aging*

Elisa Giannone
CREI

Yuhei Miyauchi
Boston University

Nuno Paixão
Bank of Canada

Xinle Pang
University at Buffalo, SUNY

Yuta Suzuki
Shanghai Jiao Tong University

June 2026

Abstract

How do depopulation and population aging evolve differently across regions within a country, and what are their implications for aggregate economic activity and regional inequality? Using spatially disaggregated data from Japan over the past several decades, we show that rural areas have experienced significantly faster depopulation and aging than urban areas, driven by low fertility and sustained out-migration of young cohorts. Regions undergoing these trends face declining local amenities and rising per-capita public service costs. To study the future evolution and economic consequences of these dynamics, we develop and calibrate a dynamic life-cycle spatial general equilibrium model. The model predicts widening geographic disparities in depopulation, aging, and economic activity in the coming centuries. While subsidies to declining regions can lower regional inequality, they come at the cost of lower aggregate efficiency and higher public service expenditures.

*We thank Jingting Fan, David Nagy, and Takaaki Takahashi for excellent discussions, as well as the seminar and conference participants at the AEA San Francisco, AMES, Atlanta Fed, Bank of Canada, Barcelona Summer Forum, Boston University, CEMFI, Chung-Ang University, Columbia University, CREI, CURE, HKUST, ICCDS, Local and International SPACE Workshops, NBER Japan Meeting, Rochester University, Rotman UToronto, SED Barcelona, Shandong University, Trasalpine Workshop, University of Bayreuth, University of Hong Kong, University of Würzburg, and World Bank for their thoughtful comments. We also thank Yilun Li for outstanding research assistance. Elisa Giannone acknowledges financial support from the Spanish Agencia Estatal de Investigación (AEI), through the Severo Ochoa Programme for Centres of Excellence in R&D (Barcelona School of Economics, CEX2024-001476-S). Yuta Suzuki acknowledges financial support from the National Natural Science Foundation of China (Grant number W2533189). The views expressed in this paper are those of the authors and do not reflect those of the Bank of Canada.

1 Introduction

Population aging and decline are major global challenges of this century. By 2050, 26 countries are estimated to have populations reduced by more than 10 percent (United Nations, 2019). Between 2015 and 2050, the proportion of the global population over 60 is projected to nearly double, reaching 22%. Academics and policy-makers have cautioned that these demographic shifts contribute to stagnating aggregate economic output and rising fiscal pressures.

Yet, an important and largely overlooked dimension of these demographic trends is their uneven spatial manifestation within countries. Aging and depopulation are often discussed in aggregate terms, which mask stark regional divergence: some locations rapidly lose their working-age populations and hollow out into so-called "ghost towns," while others remain demographically vibrant. Because economic activity is inherently local—through labor markets, amenities, housing, and local public services—heterogeneous rates of depopulation and aging can generate widening regional disparities in economic activity and welfare. Internal migration and fertility dynamics across regions play a central role in this process.

This perspective connects our setting to a broader literature documenting the "great urban divergence" of economic activity, human capital, and amenities across cities over recent decades, particularly in the United States and Europe (e.g., Berry and Glaeser, 2005; Diamond, 2016; Moretti, 2012; Hsieh and Moretti, 2015; Giannone, 2021; Combes et al., 2012). Standard explanations emphasize trade integration, skill-biased technological change, agglomeration economies, and urbanization. Much of this evidence, however, comes from economies characterized by aggregate population growth, rising urban premia, and productivity growth. Japan provides a different and useful laboratory: by 2015, aggregate population had already peaked, population aging was far advanced, and the economy had experienced a long period of low growth. The fact that younger individuals continue to concentrate in large cities in this environment suggests that spatial divergence can persist even after aggregate demographic growth has reversed.

In this paper, we study how depopulation and aging progress across regions within a country and how these processes affect welfare across regions and generations. Our context is Japan, the oldest and fastest-depopulating country. We show that rural areas have experienced significantly faster depopulation and aging than urban areas, driven by low fertility and sustained outmigration of young cohorts. Regions undergoing these trends face declining local amenities and rising per-capita public service costs. Motivated by this evidence, we develop and calibrate a dynamic life-cycle spatial general equilibrium model. The model predicts widening geographic disparities in depopulation, aging, and regional economic activity in the future. While subsidies to declining regions can generate redistributional gains, they come at

the cost of lower aggregate efficiency and higher public service expenditures.

We begin by documenting the spatial patterns of depopulation and aging in Japan over the past forty years. We show substantial spatial variation in both population aging and population decline across the country. Rural and remote areas experience faster population loss and a rapidly increasing share of elderly residents. These patterns are driven not only by differences in birth rates across regions but also by internal migration. In the most aging municipalities, the share of elderly residents has already approached nearly 50% by the early 2000s, reflecting a double burden of low fertility and the outmigration of younger cohorts, and raising the risk of municipal "extinction," as cautioned by policymakers (Masuda, 2014).

We next document substantial spatial heterogeneity in economic activity and in the cost of providing public services. To address the endogeneity of regional depopulation and aging, we adopt an identification strategy commonly used in the migration literature, exploiting variation generated by push and pull migration shocks originating in other municipalities (e.g., Boustan (2010), Derenoncourt (2022), and Bazzi et al. (2023)). We find that depopulating areas tend to experience a decline in local amenities, including the availability of retail and medical services, suggesting a deterioration in local quality of life. At the same time, these areas exhibit higher government spending per capita, consistent with the higher per-capita costs of public service provision in shrinking regions.

Motivated by this empirical evidence, we develop a quantitative dynamic spatial general equilibrium model to analyze the underlying drivers of these trends and their implications for future demographic patterns and policy. In each period, individuals make forward-looking migration decisions across locations within the country, based on wages, amenities, housing costs, and migration costs. Wages and amenities are endogenously determined by the local population through agglomeration externalities. The national government collects taxes on labor income to finance pensions for the elderly and to provide the required level of local public services, which vary with local population size. Individuals of reproductive age give birth in their current locations, generating the next cohort of the population.

We calibrate the model to match Japanese data in 2015 so that it replicates the observed regional patterns of depopulation and aging. We then use the calibrated model to assess whether these divergent regional trends are likely to persist in the future. Our simulations predict that they will continue for the next 200 years. In particular, the population of Tokyo prefecture continues to expand, rising from about 10 percent of Japan's population in 2015 to roughly 25 percent over the next 200 years, largely by drawing population from more remote prefectures. While the share of elderly residents in Tokyo remains below 35 percent, the corresponding share in the five oldest prefectures continues to rise, reaching nearly 60 percent after 200 years.

We show that these dynamics are driven jointly by internal migration and the spatial distribution of births. If we shut down internal migration, or alternatively assume that the spatial distribution of newborns remains fixed at its 2015 level (and hence it is not affected by the spatial distribution of the reproductive population), regional population shares remain constant rather than diverging. In this case, the fraction of elderly residents also converges across regions instead of continuing to diverge.

We further document that these demographic patterns have important implications for spatial inequality and aggregate efficiency. In particular, flow utility (amenity-adjusted real income) will continue to diverge, rather than converge, between Tokyo and rural prefectures. This divergence is driven primarily by the continuing population concentration in Tokyo and the associated agglomeration externalities. As a result, spatial inequality in economic well-being is expected to widen, even though the share of the population living in rural areas gradually declines. When internal migration is shut down or the spatial distribution of newborns is fixed at the 2015 level, regional population shares remain constant and the gap in real income across regions remains unchanged. However, these counterfactual scenarios also reduce aggregate per capita income and increase per capita fiscal spending, as they keep a larger share of the population in less productive rural locations, where the provision of public services is more costly.

These findings imply that policymakers face an efficiency–equity trade-off. On the one hand, the continued depopulation and aging of rural areas raise concerns about spatial inequality and may justify redistributive policies targeting these regions. On the other hand, such redistribution may encourage the population to remain in or move toward less productive locations with higher public service costs.

In the final section of the paper, we quantify this trade-off by simulating monetary transfers to residents of depopulated and aging regions, financed through taxes levied on residents of Tokyo. We find that these transfers have substantial long-run effects on population distribution. For example, committing to transfers equal to 5 percent of income for the next 100 years toward the five oldest prefectures would nearly double the population of those areas in 2065 relative to the baseline prediction without transfers, while reducing the share of elderly residents from 45 percent to about 33 percent. Real income in these areas increases by about 10 percent, which is larger than 5 percent of the transfer rates, reflecting amplification through agglomeration externalities. By contrast, income in Tokyo declines by about 3 percent, a much smaller effect due to its larger population base. At the same time, at the national level, aggregate labor income per capita falls by more than 1 percent and aggregate fiscal spending rises by 0.5 percent, reflecting the efficiency losses associated with redistributive policies and the induced reallocation of population toward less productive locations.

Overall, our analysis suggests that the regional dimension of depopulation and aging is, and will continue to be, as important as the aggregate trend. Policies aimed at addressing depopulation and aging in rural areas must therefore carefully weigh the trade-off between redistributional gains and efficiency losses.

This paper connects to three main strands of literature. First, it contributes to the study of the economic consequences of depopulation and aging. While existing work has examined the aggregate effects of nationwide demographic change, both empirically and theoretically, much less is known about how these processes unfold across regions within a country.[1] In the context of Japan, Braun and Joines (2015); Kitao (2015) and Kitao and Mikoshiba (2020) study the implications of nationwide aging and depopulation for labor markets and fiscal policy using lifecycle overlapping-generations (OLG) models, abstracting from regional heterogeneity. In contrast, our paper emphasizes the regional dimension, highlighting the roles of internal migration and fertility dynamics in shaping spatial demographic dynamics.

Second, we contribute to the urban and regional literature on spatial divergence across cities. A large body of work documents the increasing concentration of skilled workers, productivity, and amenities in large cities, and relates these patterns to skill-biased technological change, agglomeration economies, and housing-market constraints (e.g., Berry and Glaeser, 2005; Diamond, 2016; Moretti, 2012; Hsieh and Moretti, 2015; Giannone, 2021; Combes et al., 2012). Our contribution is to study whether similar forces operate in a setting where aggregate population growth has ended and population aging is already advanced. Earlier work by Gaigné and Thisse (2009) and Takahashi (2022) uses stylized theoretical models to examine how migration and fertility shape depopulation and aging patterns. In contrast, we combine spatially disaggregated data with a quantitative model that can be disciplined by the data to simulate future scenarios and quantify the effects of policies. Mori and Murakami (2025) constructs a statistical model to project population dynamics in Japan; by contrast, our microfounded economic framework enables us to analyze implications for both local and aggregate economic outcomes, as well as policy counterfactuals.

Several recent papers employ related quantitative spatial lifecycle models to study migration and spatial sorting over the life cycle (Giannone et al., 2020; Komissarova, 2022), the consequences of labor market shocks (Suzuki, 2023), quality of life over the lifecycle (Ahlfeldt et al., 2025), and fertility decisions (Moreno-Maldonado and Santamaria, 2022; Arkolakis et al., 2026). Relative to these studies, our focus is on understanding the causes and consequences of regional heterogeneity in depopulation and aging. Our empirical analysis also resonates with Badilla Maroto et al. (2026), which studies the local economic effects of an influx of

[1] For example, prior studies analyze the impact of population decline on economic growth (Acemoglu and Restrepo, 2022; Jones, 2022), business dynamism (Karahan et al., 2019; Hopenhayn et al., 2021; Engbom, 2019), and wealth distribution (Auclert et al., 2025).

pensioners in France.

Third, our project contributes to the literature on the design of place-based policies, particularly work highlighting the trade-off between spatial redistribution and efficiency in both static spatial equilibria (Fajgelbaum and Gaubert, 2020; Gaubert et al., 2021; Davis and Gregory, 2021; Ales and Sleet, 2022; Mongey and Waugh, 2024; Donald et al., 2026) and dynamic spatial equilibria (Donald et al., 2025). Our quantitative analysis illustrates this trade-off in the context of population decline and aging.

The rest of this paper proceeds as follows. In Section 2, we provide an overview of Japan's demographic transition and describe our data sources. In Section 3, we document spatial patterns of depopulation and aging in Japan and how they have affected the local economy. In section 4, we develop a dynamic life-cycle spatial equilibrium model. In Section 5, we calibrate our model to the population and migration data from Japan. In Section 6, we use our calibrated model to project future spatial patterns of depopulation and aging and discuss its welfare implications. Section 7 will analyze the impacts of place-based transfers. Section 8 concludes.

2 Background and Data

2.1 Depopulation and Aging in Japan

Japan is one of the most depopulating and aging countries in the world. Japan's total population began to decline around 2010 and is expected to shrink by nearly 20 percent relative to its 2010 level by mid-century (left panel, Figure 1). As of 2015, it had the highest share of elderly individuals in the world: 26 percent of the population was aged 65 or older, a figure projected to rise to 37 percent by 2050 (right panel, Figure 1). These aggregate trends are driven primarily by rising life expectancy and persistently low fertility.[2]

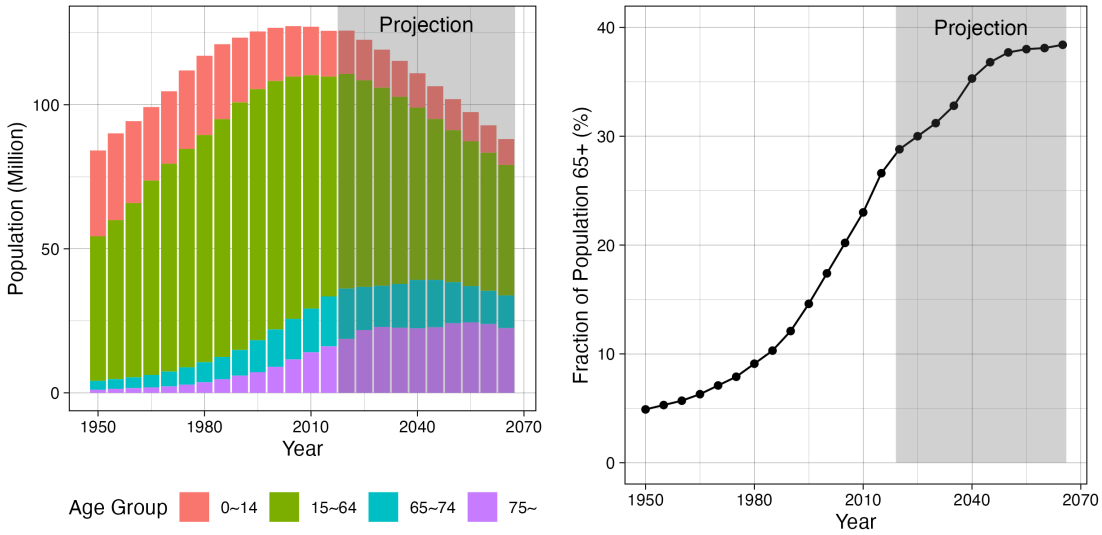
At the same time, there is substantial cross-sectional dispersion in both population density and aging across regions in Japan. The left panel of Figure 2 plots population density across municipalities in 2010, revealing large dispersion. Municipalities surrounding major metropolitan areas—such as Tokyo, Osaka, and Nagoya—exhibit densities far above the average (median) of roughly 1,000 (200) persons per square kilometer, while rural areas are sparsely populated.

The right panel of Figure 2 shows equally pronounced variation in aging, measured as the share of the population aged 65 and above. Municipalities near major metropolitan areas

[2]See Appendix Figure B.1 for the aggregate changes in life expectancy and fertility rates. International migration plays only a limited role in Japan, as both inflows and outflows have historically been small relative to other advanced economies.

Figure 1: Aggregate Patterns of Depopulation and Aging in Japan

(a) Population Decomposition by Age (b) Fraction of Population above 65 Years Old

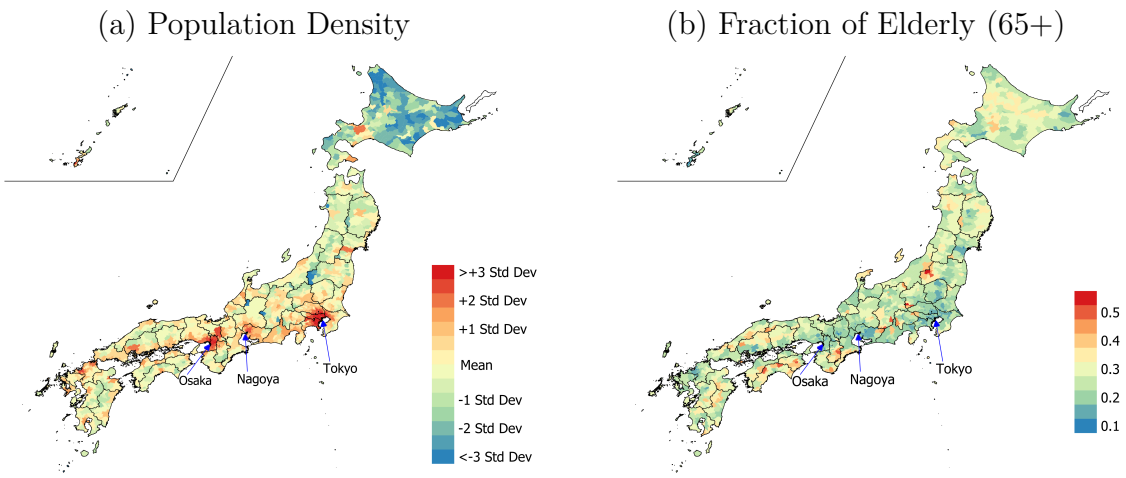


Note: Figure 1 plots aggregate patterns of depopulation and aging in Japan. Data through 2015 are drawn from the Population Census, and data for 2020 are from the Population Estimates of the Ministry of Internal Affairs and Communications. Data from 2025 onward are based on population projections from the National Institute of Population and Social Security Research (2017 projection, medium-fertility and medium-mortality assumptions), covering the period through 2065.

tend to have relatively low elderly shares, typically between 10 and 20 percent, whereas rural municipalities exhibit substantially higher levels, some reaching 50 percent. Consistent with this pattern, Figure 3 shows that municipalities with higher population density indeed tend to have a lower share of elderly residents.

These patterns raise a natural question: how do depopulation and aging evolve across regions? How are these dynamics linked to migration, fertility, and economic activity? We address these questions by assembling spatially disaggregated data on Japanese population dynamics and economic activity over the past several decades.

Figure 2: Heterogeneity of Population Density and Aging across Municipalities in Japan

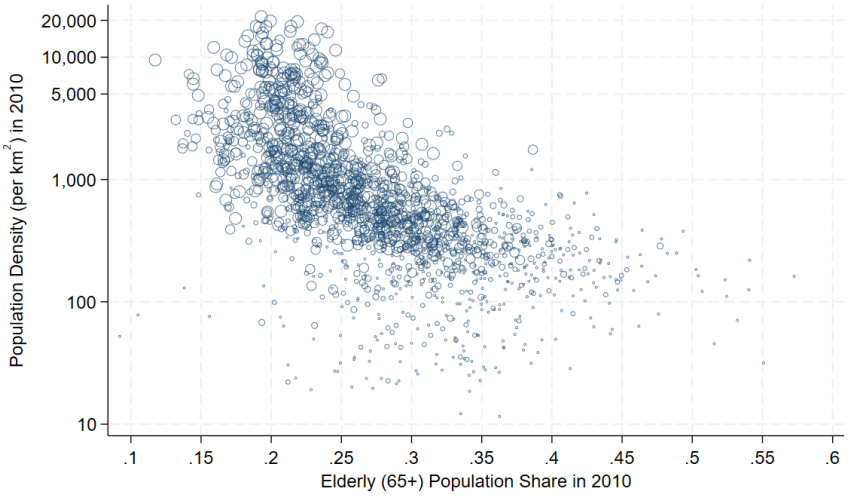


Note: Figure 2 maps population density and the share of the population aged 65 or above across municipalities in 2010. The solid black border indicates prefecture boundaries. See Figure B.2 for the corresponding distributions across municipalities.

2.2 Data Sources

Before we introduce our data source, we describe the geographic units of our analysis. Japan is divided into 47 prefectures. Each prefecture is further divided into municipalities. There are 1741 municipalities in Japan as of 2015. The average geographic size of the municipality is around 220 square kilometers. The average population size is 72,000, with substantial heterogeneity in population size, as noted above. The number of municipalities has significantly decreased over the last 20 years due to municipality mergers. To keep the spatial units of our analysis consistent across years and unaffected by municipal mergers, we use the crosswalk of municipalities across years in Japan developed by Kondo (2019) and use the municipal spatial unit in 2015. For our reduced-form analysis in Section 3, we take municipalities as

Figure 3: The Relationship between Population Density and Aging Across Municipalities



Note: Figure 3 shows the relationship between population density and the share of the elderly population (aged 65 or above) in 2010 at the municipality level. Municipalities are grouped into five categories based on population size, and bubble sizes are scaled to reflect these groups. Population density is calculated using habitable land area.

the spatial unit of the analysis. For our quantitative analysis in Section 4 onward, we use prefectures as our spatial unit.

Below, we describe the data sources we assemble for our analysis. Appendix Table A.1 summarizes the source and available spatial units for each data source.

Population Census. Population censuses in Japan are conducted every 5 years by the Statistics Bureau of the Ministry of Internal Affairs and Communications (MIC). The population censuses collect each individual's demographic characteristics (e.g., age, gender), employment status and sector, and the current residential location. Furthermore, every 10 years since 1990 (and every 5 years after 2010), the population censuses also collect information on where each individual resided 5 years ago. Based on current residence and residence 5 years earlier, publicly available statistics provide municipality-to-municipality flows over the preceding 5-year window, from 1990 for the total population and from 2015 onward by age group. We use this information to extract migration flows. Lastly, we use information on employment status by age, gender, and municipality to calibrate our model.

Vital Statistics. Vital statistics are collected annually by the Ministry of Health, Labor, and Welfare. This data reports the number of births for each prefecture, disaggregated by mothers' age. We construct fertility rates by parents' age for each prefecture using this

information. This data also reports the number of deaths for each prefecture disaggregated by age and gender. We construct age- and gender-specific mortality rates for each prefecture using this information.

Projected Fertility and Mortality Rates. We use national-level fertility and mortality rates reported by the National Institute of Population and Social Security Research (IPSS) in its Population Projections for Japan (2017 Revision). The data include observed values for 2015 and projected values from 2020 onward, covering the period through 2065. We use these projections to conduct the future projection using our calibrated model.

Taxable Income and Local Government Spending. We measure the average taxable income of the residents in each municipality using official data on the tax base for that municipality collected by the Ministry of Internal Affairs. We use data on local government spending at the municipal level from the Survey of Municipal Fiscal Accounts and data on total government spending at the national level from the Ministry of Finance.

Basic Survey on Wage Structure. We extract information about wages by gender and age group from the Basic Survey on Wage Structure. It is an annual survey conducted on a random sample of establishments across Japan by the Ministry of Health, Labor, and Welfare. This data is available at the prefecture level. We extract average wages for each prefecture, age group, gender, and occupation. We use this information for calibrating our model.

Housing Stock and Land Prices. We use data on the housing stock, including the number of dwellings and housing construction, from the Housing and Land Survey, a household survey conducted every five years by the Statistics Bureau of the Ministry of Internal Affairs and Communications. We measure the changes in land prices using the official posting of land prices of designated plots across Japan posted by the Ministry of Land, Infrastructure, Transport and Tourism. For each plot, the data reports the evaluated land prices based on the characteristics of the plot and the surrounding environment. This data is typically used as a reference for property tax collection and land transactions.

Amenity Index. We collect various proxies for residential amenities. For our purpose, we classify these amenities into five categories: (1) child/education (number of daycares, libraries, schools, and teachers); (2) elderly service (number of community centers, nursing homes, and senior citizen clubs); (3) environment/transportation (number of parks, paved road length, number of police stations, and road length); (4) health/medical (number of clinics, general hospitals, medical doctors, and nurses); and (5) retail (number of auto retail stores,

beauty salons, clothing stores, food and beverage retail stores, large retail stores, restaurants, and retail stores). Following Diamond (2016), for each category, we create an index using principal component analysis (PCA). Appendix Table A.2 reports the loading coefficients of each variable within each category.

3 Reduced-Form Evidence

In this section, we document Japan's spatial pattern of depopulation and aging and how it has affected the local economy.

3.1 Regional Heterogeneity in Depopulation and Aging

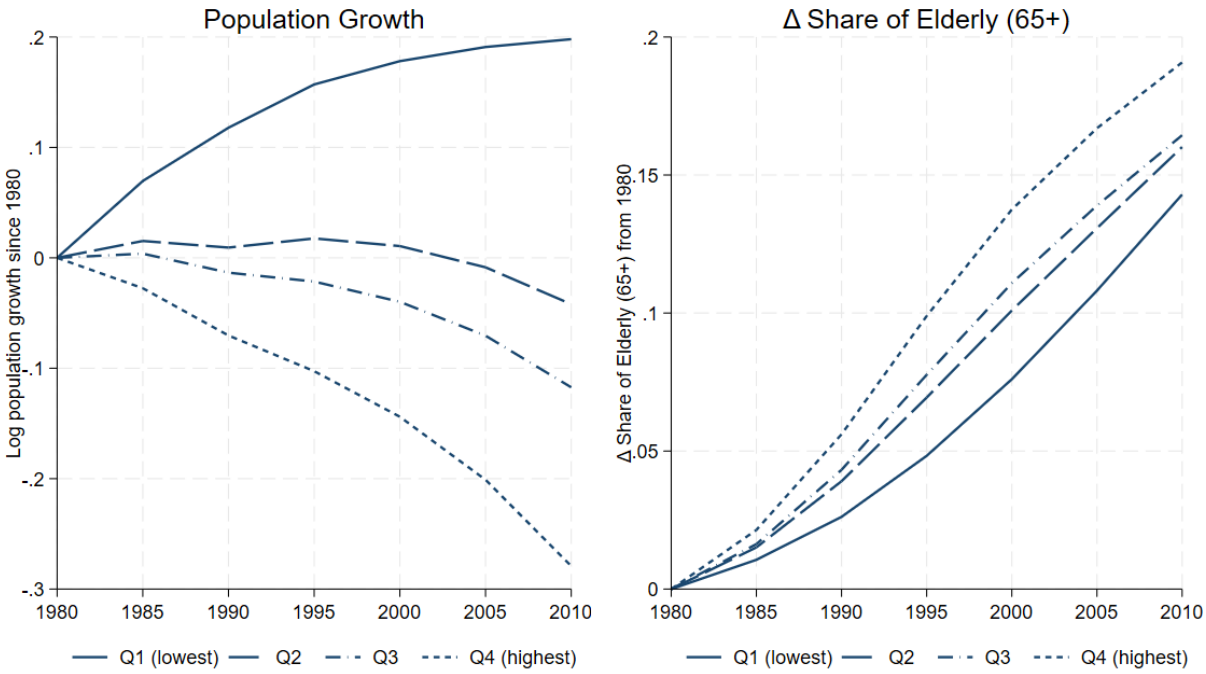
We begin by documenting the spatial patterns of depopulation and population aging in Japan since 1980. Figure 4 shows changes in population size (left panel) and in the share of the elderly (right panel) between 1980 and 2010. Each line reports the average outcome for municipalities grouped into quartiles based on their initial share of elderly residents (age 65 and above), which closely tracks population density, as discussed in Figure 2.

The figure reveals a clear pattern of divergence in both population and age structure. Between 1980 and 2010, municipalities in the youngest quartile experienced population growth of nearly 0.2 log points, while those in the oldest quartile saw population decline of nearly 0.3 log points. Strikingly, the gap between these groups widens over time rather than narrowing, reflecting an accelerating divergence. A similar pattern appears in the right panel: the share of elderly residents increases more rapidly in municipalities that already had higher elderly shares in 1980, further amplifying spatial differences in aging.

Figure 4 provides the within-Japan demographic counterpart to the urban-divergence patterns discussed above. The divergence here is not measured by wages, skills, or productivity, but by population growth and age structure: municipalities that were already relatively young in 1980 grow and remain younger, while initially older municipalities shrink and age faster. This distinction matters because Japan was moving toward aggregate population stagnation and decline over this period. The evidence therefore suggests that spatial divergence can be reinforced by demographic forces even when national population growth is weak, motivating the decomposition below into migration and the spatial distribution of births.

Following the demographic literature (Smith et al., 2006, 2013), the differential rates of depopulation and aging can be attributed to two distinct margins. The first is "social population change," which reflects population movements through in- and out-migration. The second is "natural population change," which arises through the process of births and deaths.

Figure 4: Depopulation and Aging across Municipalities



Note: Figure 4 reports changes in population size and in the share of the elderly population over five-year intervals from 1980 to 2010. Each line reports the average outcome for municipalities grouped into quartiles based on their initial share of the elderly population (aged 65 or above), with Q1 representing the lowest share and Q4 the highest. All changes are measured relative to their 1980 levels.

To illustrate the role of these two margins, we conduct two simple accounting exercises.

In the first experiment, we isolate the role of social population change by constructing a counterfactual population path under the assumption of no migration across municipalities. Let $L_t^n(a)$ denote the observed population of age group a in municipality n in year t, where age groups are defined in five-year intervals from 0–4 to 100+. We denote the hypothetical population abstracting migration by $L_t^{n,\text{nomig}}(a)$, which is constructed sequentially starting from $t = 1980$ as

$$L_t^{n,\text{nomig}}(a) = s_{t-5}(a-5)L_{t-5}^{n,\text{nomig}}(a-5), \tag{1}$$

with initial condition $L_{1980}^{n,\text{nomig}}(a) = L_{1980}^n(a)$, where $s_{t-5}(a-5)$ denotes the national survival rate from $t-5$ to t for age group $a-5$.[3] For newborns in each period, we use the observed

[3]We assume homogeneous survival rates across municipalities for this exercise, consistent with its limited spatial variation in Japan (Appendix Figure B.4).

population, $L_t^{n,\text{nomig}}(0) = L_t^n(0)$.

In the second experiment, we isolate the role of natural population change by assuming that the spatial distribution of newborns remains fixed at its 1980 level. In reality, this distribution evolves over time because the size of the reproductive-age population and fertility rates vary across regions.[4] Fixing the spatial distribution of newborns shuts down this source of variation. We denote by $L_t^{n,\text{birth}}(a)$ the resulting hypothetical population. For newborns ($a = 0$), we set

$$L_t^{n,\text{birth}}(0) = \left(\frac{L_{1980}^n(0)}{B_{1980}} \right) B_t, \tag{2}$$

where $B_t \equiv \sum_n L_t^n(0)$ is the total newborn in period t within Japan. Therefore, we hypothetically reallocate the newborns' locations using their observed share in 1980, regardless of their actual parents' location. For all other age groups, we impute using the observed population growth rates for each location, time, and age, starting from 1980:

$$L_t^{n,\text{birth}}(a) = \left(\frac{L_t^n(a)}{L_{t-5}^n(a)} \right) L_{t-5}^{n,\text{birth}}(a-5), \tag{3}$$

with initial condition $L_{1980}^{n,\text{birth}}(a) = L_{1980}^n(a)$.

Figure 5 shows the change in population for municipalities in the least-aging quartile (left panel) and the most-aging quartile (right panel) as of 1980. The figure reports the observed data (solid line) together with the two counterfactual experiments (dashed and dash–dot lines). As discussed in Figure 4, municipalities in the youngest quartile experienced population growth of about 0.2 log points between 1980 and 2010, whereas those in the oldest quartile lost nearly 0.3 log points of their population.

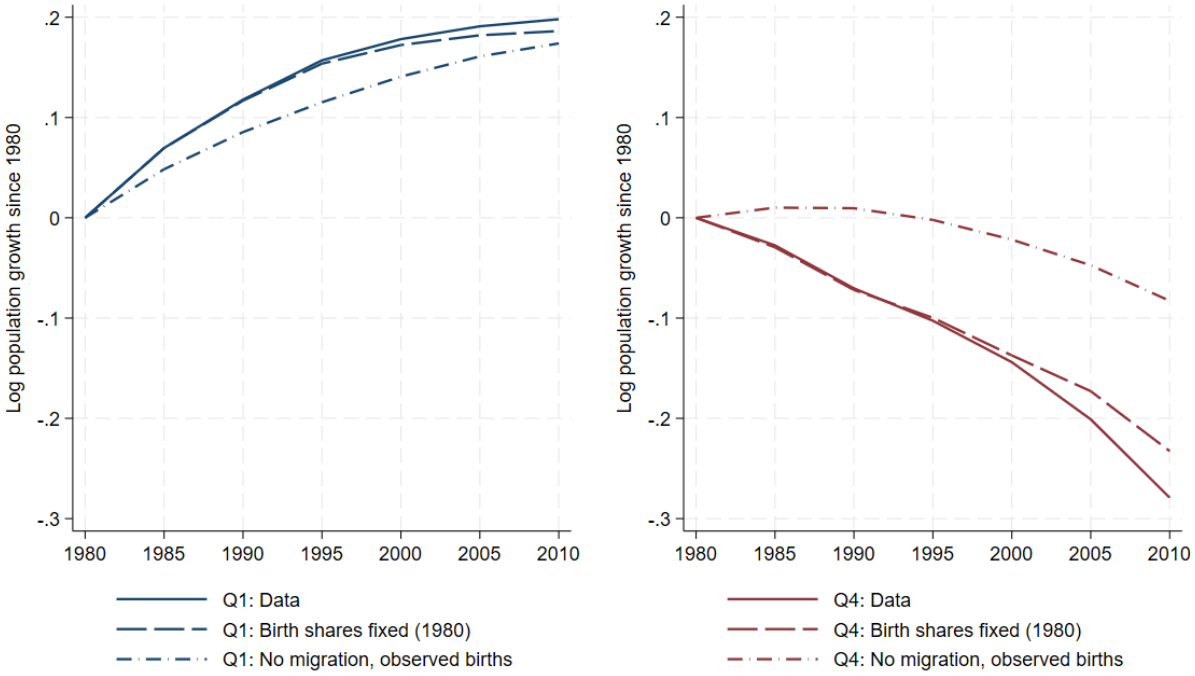
When we shut down internal migration ("No migration, observed births"), this gap narrows substantially, primarily because population decline becomes much slower in the oldest municipalities. In this counterfactual, the population loss in the oldest quartile would have been less than 0.1 log points, rather than the nearly 0.3 log points observed in the data.[5]

When we shut down changes in the spatial distribution of births ("Birth shares fixed"),

[4] In Appendix B.5, we show that most of the spatial variation in the newborn population is explained by the spatial distribution of the reproductive-age population. While fertility rates per reproductive age population do vary across regions (Appendix Figure B.5), their contribution to the spatial distribution of newborns is small compared to the former variation.

[5] Supporting the importance of migration in the counterfactual decomposition, Appendix Figure B.3 shows that municipalities in the youngest quartile consistently experience positive net in-migration, while municipalities in the older quartiles experience net out-migration. Although migration rates attenuate somewhat after 1990, the overall pattern remains similar throughout the period, particularly after 2000. This suggests that internal migration continued to contribute to population concentration in younger municipalities both before and after Japan entered a phase of population decline around 2010.

Figure 5: Depopulation across Municipalities: Accounting for Social and Natural Population Changes



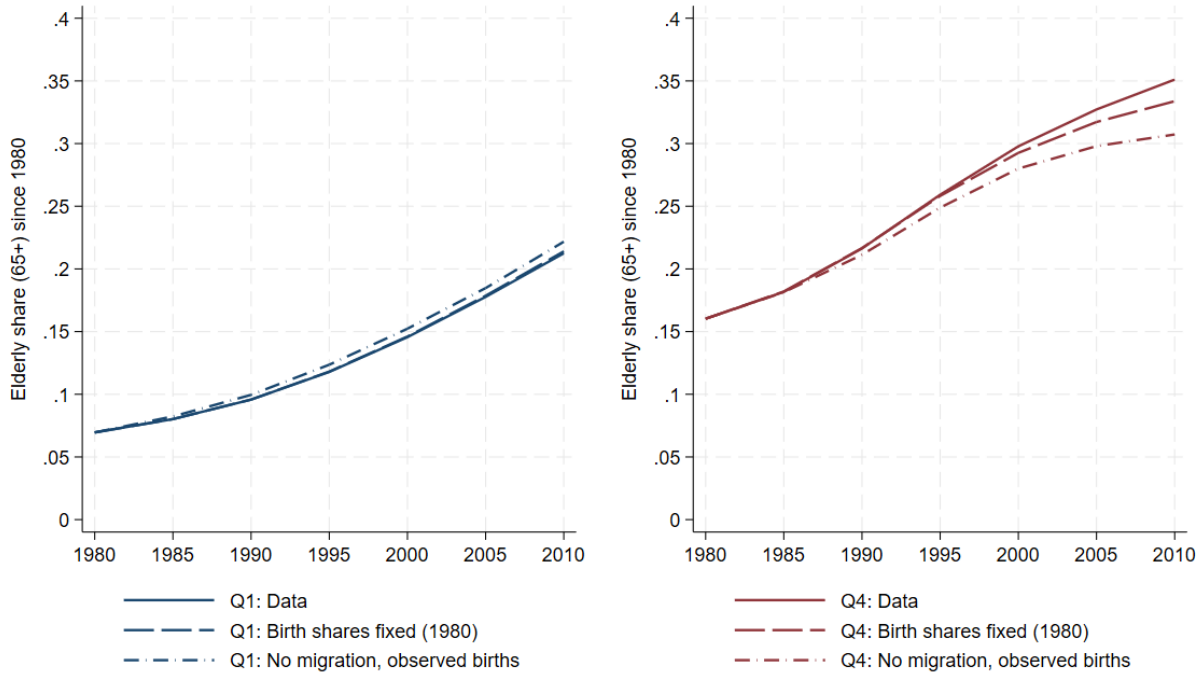
Note: Figure 5 shows observed changes in population size (in logs) ("Data"), a counterfactual in which newborns are redistributed across regions according to birth shares in 1980 ("Birth shares fixed (1980)"), and a counterfactual that shuts down migration, projecting population changes based solely on births (as observed) and deaths (computed using national mortality rates). The left panel reports the average outcomes for Q1 municipalities (those with the lowest elderly share in 1980), while the right panel reports the corresponding outcomes for Q4 municipalities (those with the highest elderly share).

the gap also narrows, while the paths remain closer to the baseline, especially in the short run. This is partly mechanical, as spatial birth patterns evolve slowly. However, the gap between the baseline and this counterfactual gradually widens over time, because the reproductive age population has become more and more concentrated in central municipalities over time. Therefore, shifts in the spatial distribution of births accumulate and contribute to the continued regional divergence in depopulation rates over a longer-time horizon.

Figure 6 presents the results of the same decomposition for the fraction of the elderly. In the baseline, the share of elderly residents in the youngest municipalities starts at around 7% and rises to above 20% by 2010. In contrast, in the oldest municipalities the share begins at about 16% and increases to over 35% during the same period. As a result, regional disparities in the elderly share widen rather than converge over time.

When we shut down internal migration, this gap becomes smaller. In particular, the elderly share in the oldest municipalities would reach about 30% by 2010, roughly five percentage points lower than in the baseline. This pattern reflects the fact that migrants tend to be younger on average: the outmigration of younger cohorts accelerates population aging in already older regions. Shutting down changes in the spatial distribution of births also reduces the gap, especially in the longer run, indicating that persistent shifts in where newborns are born further contribute to the divergence in regional aging patterns.

Figure 6: Aging across Municipalities: Accounting for Social and Natural Population Changes



Note: Figure 6 shows observed changes in the share of the elderly population (aged 65 or above) ("Data"), a counterfactual in which newborns are redistributed across regions according to 1980 birth shares ("Birth shares fixed (1980)"), and a counterfactual that shuts down migration, with changes in the elderly share driven solely by births (as observed) and deaths (computed using national mortality rates). The left panel reports average outcomes for Q1 municipalities (those with the lowest elderly share in 1980), while the right panel reports the corresponding outcomes for Q4 municipalities (those with the highest elderly share).

3.2 The Impacts of Depopulation and Aging on Local Economy

We next examine how local depopulation and aging affect economic outcomes. In particular, we study how local economic conditions respond to these demographic changes using the

following regression specification:

$$\Delta \log Y^n = \beta_1 \Delta \ln Pop(age \in [15,64])^n + \beta_2 \Delta \frac{Pop(age \geq 65)^n}{Total\ Pop^n} + \boldsymbol{X}^n_{1980}\boldsymbol{\beta} + PrefFE^n + \varepsilon^n, \tag{4}$$

where n indicates the municipality; Δ indicates the long difference between 1980-2010 (or the closest years depending on the availability of outcome variables); $\Delta \log Y^n$ are a set of outcome variables that proxy for the changes in local economic activity (e.g., amenity, local fiscal spending, land prices); and $PrefFE^n$ denotes prefecture fixed effects, which we include to control for broader regional trend. The variable $\Delta \ln Pop(age \in [15,64])^n$ captures the growth rate of the working-age population density, defined using habitable land area, while $\Delta \frac{Pop(age \geq 65)^n}{Total\ Pop^n}$ measures the change in the elderly share. The vector $\boldsymbol{X}^n_{1980}$ includes a set of pre-period controls: employment shares in the secondary and tertiary sectors, total land area (in logs), total population density (in logs), the ratio of habitable land area to total land area (in logs), the share of elderly, the share of children (under age 15), and the skilled-to-unskilled ratio (in logs, where skilled workers are defined as college graduates or above), all measured in 1980, as well as taxable income per capita (in logs) in 1985.

A key endogeneity concern of this specification is that unobserved factors related to the changes in local economic conditions, captured by ε^n, may be associated with the changes in local population. For example, regions experiencing an economic boom may attract working-age population, rather than the other way around. Similarly, regions with improved amenities for the elderly, such as an increase in nursing homes or senior citizens clubs, may attract an inflow of the elderly.

To address these concerns, we follow the literature on the consequences of internal migration on the local labor market (e.g., Boustan (2010), Derenoncourt (2022) and Bazzi et al. (2023)) to construct instrumental variables (IV) based on age-specific push and pull migration shocks from other municipalities within Japan. The basic idea for push migration IV is to predict the in-migration to municipality n solely from the predetermined migration patterns in the baseline period (1980) and the fact that municipalities that tend to send population to municipality n experience an overall out-migration (not specifically to destination n) during 1980-2010. For example, if a municipality n tends to receive a large inflow of migrants from a municipality i of a specific age group, and if municipality i happens to experience an outflow of this population (for example due to the economic decline in municipality i), municipality n is likely to experience an increase in in-migration of this specific age group. The idea for the pull migration shock is similar: We predict the out-migration from municipality n solely from the predetermined migration patterns in the baseline period (1980) and the fact

that municipalities that tend to receive population from municipality n experience an overall in-migration (not specifically from origin n) during 1980-2010.

Following this idea, we construct our push IV based on the cumulative hypothetical inflows for age group a in municipality n in 2010 from the push migration shocks, starting from 1980, as follows:

$$\tilde{\mathcal{I}}^d(a) = \sum_{o \neq d} \sum_{s=1985,1995,2005} \tilde{\mu}^{od}_{1980}(\tilde{a}_s(a)) \mathcal{O}^o_s(\tilde{a}_s(a)), \tag{5}$$

where $\mathcal{O}^o_s(a)$ indicate the observed outflow of age group a in municipality n in year s to $s+5$; 1985, 1995, 2005 are the years where we observe those information from our census data; and $\tilde{\mu}^{od}_{1980}(a)$ indicates the share of out-migrants from municipality o going to municipality d from 1980 to 1985. The function $\tilde{a}_s(a)$ maps age group a in 2010 to the corresponding age group in year s. For example, individuals aged 25–29 in 2010 correspond to ages 10–14 in 1995 and 20–24 in 2005. If a cohort has not yet been born in year s, its contribution is set to zero. Thus, out-migration shocks at time s for cohort $\tilde{a}_s(a)$ contribute to the size of cohort a in 2010.

Similarly, we construct our pull IV based on the cumulative hypothetical outflows for age group a in municipality n in 2010 from the pull migration shocks, starting from 1980, as follows:

$$\tilde{\mathcal{O}}^o(a) = \sum_{d \neq o} \sum_{s=1985,1995,2005} \breve{\mu}^{od}_{1980}(\tilde{a}_s(a)) \mathcal{I}^d_s(\tilde{a}_s(a)), \tag{6}$$

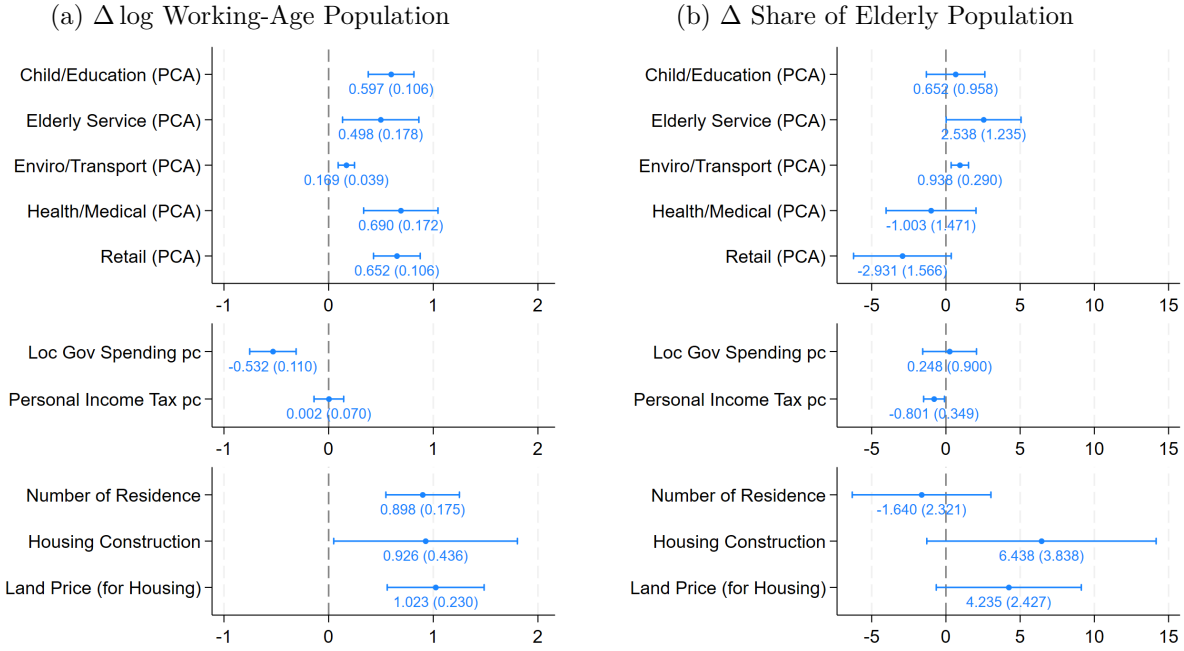
where $\mathcal{I}^d_s(a)$ indicates the observed inflow of age group a in municipality d in year s to $s+5$; and $\tilde{\mu}^{od}_{1980}(a)$ indicates the share of in-migrants to municipality d coming from municipality o from 1980 to 1985.

After constructing $\tilde{\mathcal{I}}^d(a)$ and $\tilde{\mathcal{O}}^o(a)$, we aggregate these quantities across age groups to obtain predicted changes in the working-age and elderly populations attributable to push and pull shocks, respectively, for each municipality. We then transform these predicted changes into percentiles and use them as instruments for the first two regressors in equation (4).

In implementing this IV approach, we use the projected initial migration shares for $\tilde{\mu}^{od}_{1980}(\tilde{a}_s(a))$ and $\breve{\mu}^{od}_{1980}(\tilde{a}_s(a))$, instead of actual one, since age-specific bilateral migration flows are not available for 1980. Specifically, we parametrize migration costs as a function of geographic variables, such as geographic distance and prefecture borders, and estimate this parametric costs using observed bilateral migration data in 2015. We then use population distributions by age groups and municipalities in 1980 and 1985 to construct the predicted initial migration flows. Appendix B.2 describes the details of this procedure.

Figure 7 shows the regression coefficients of the IV specification (4). Panel (a) shows the coefficients and the 95% confidence intervals on the log change in the working-age population size for each outcome variable indicated in the horizontal axis, and Panel (b) shows those on the change in the share of elderly. All variables except for amenity proxies are defined as log changes.

Figure 7: Impacts of Depopulation and Aging on Local Economy



Note: Figure 7 reports coefficient estimates from equation (4), where each dependent variable is the change in a local economic outcome. The left panel shows the coefficients on Δ log working-age population, while the right panel shows the coefficients on Δ share of the elderly population. Horizontal bars indicate 95% confidence intervals for the reported estimates. All variables, except the amenity proxies in the top panel, are expressed as log changes. For the amenity proxies, we standardize their growth rates to have a standard deviation of one. See Appendix B.3 for the estimated impacts on the underlying variables within each amenity category. The corresponding regression results and first-stage estimates are reported in Appendix B.4.

The top panel reports the effects on the PCA indices for five categories of amenities: (1) Child/Education, (2) Elderly Services, (3) Environment/Transportation, (4) Health/Medical, and (5) Retail, as defined in Section 2. To facilitate the interpretation of the magnitudes, we standardize the growth rates of these proxies to have a standard deviation of one.

Across all categories, the coefficients on working-age population are positive and statistically significant (left panel). This implies that amenities decline in areas experiencing population loss. The results are consistent with a mechanism in which the supply of amenities responds endogenously to local market size (e.g., Diamond, 2016). Together, these patterns suggest that the economic well-being of residents remaining in depopulating areas deteriorates over time.

By contrast, the coefficients on the share of the elderly tend to be insignificant (right panel), with the exception of category (2) Elderly Services, and (3) Environment/Transportation.

The middle panel reports the effects on average government spending and personal income tax per capita. We find that a one percent increase in population is associated with a 0.53 percent decrease in local (municipality) government spending per capita. This pattern suggests the presence of scale economies in the provision of local public services, implying that maintaining public services becomes increasingly costly on a per-capita basis in shrinking regions. In contrast, personal income tax per capita—which includes both labor and capital income of residents—shows no statistically significant response to changes in working-age population size. The local government spending per capita is not strongly associated with the share of the elderly population, while the personal income tax per capita is negative and marginally significant, reflecting lower taxable income for the elderly population.[6]

The bottom panel reports the effects on housing markets and land prices. We find that growth in the working-age population has a significantly positive effect on both land prices and the number of residences, suggesting that part of the amenity value is capitalized into land prices. We also find that the share of the elderly has a negative effect on the number of residences and a positive effect on housing construction and land prices. However, the coefficients on the first two outcomes are not statistically significant, and the effect on land prices is only marginally significant.[7]

Overall, these findings point to widening economic disparities across regions experiencing different rates of depopulation. Areas with rapid population decline face deteriorating local amenities and lower government spending per capita, consistent with the higher per-capita costs of providing public services in shrinking regions.

4 A Dynamic Spatial Model of Depopulation and Aging

In this section, we develop a dynamic spatial model of depopulation and aging that captures the observed geographic patterns of these processes. We use the model to analyze their future evolution, assess their economic consequences, and evaluate the implications for place-based transfer policies.

The economy consists of a finite set of locations, indexed by $i \in N$. Time is discrete and indexed by $t = 0, 1, 2, \ldots$. Individuals are indexed by age $a \in 0, 1, \ldots, \bar{a} \equiv A$. In each period,

[6]Pension payments are classified as taxable income under the Japanese taxation scheme.

[7]Changes in land prices are constructed using the official posted prices of designated plots within each municipality. Specifically, controlling for plot fixed effects, we regress log land prices on municipality-year fixed effects and take the difference of the fixed effects between 1980 and 2010 as the estimated change in land prices of that municipality.

agents age from a to $a+1$ until reaching the terminal age group $\bar{a}$. Agents who reach this terminal age group $\bar{a}$ remain there until they die stochastically. Survival probabilities are age-, location-, and time-dependent and given by $s_t^n(a)$. We denote by $L_t^i(a)$ the population of age a residing in location i at time t.

Within each period t, the following events happen in order. First, households of age a give birth in location n with probability $\varkappa_t^n(a)$, thereby generating newborns $L_t^i(0)$. Next, agents supply labor, receive income, and allocate it between consumption of the final good and housing. Next, households decide where to live in the next period. Finally, the death shock realizes.

Individuals below the minimum working age $\underline{a}$ do not participate in the labor market, do not consume, and simply stay in their birth location. Agents begin to receive pensions at age a^*, which also defines the threshold above which individuals are classified as elderly (set to 65 in our quantification).

4.1 Households

The flow utility of an agent of age $a \geq \underline{a}$ at time t in location n is given by :

$$u_t^n\left(c_t^n(a), h_t^n(a), \chi_t^n(a)\right) = (1-\theta)\ln c_t^n(a) + \theta \ln h_t^n(a) + \ln \chi_t^n(a) \tag{7}$$

where $c_t^n(a)$ denotes the consumption of the final good that is freely traded across regions, and we normalize its price to one as a numeraire. $h_t^n(a)$ represents housing consumption, which can be rented at R_t^n per unit. The term $\chi_t^n(a)$ captures the amenity value of location n for age group a at period t.[8] The amenity value has two components: an exogenous component, which is location- and age-specific and reflects inherent characteristics such as proxy to the ocean, rivers, or forests; and an endogenous component, which depends on the local working population size, such that

$$\ln \chi_t^n(a) = \ln \tilde{\chi}_t^n(a) + \gamma^a \ln L_t^{n,W}, \tag{8}$$

where $L_t^{n,W}$ denotes the size of the working-age population in location n, $L_t^{n,W} = \sum_{a\in[\underline{a},a^*]} L_t^n(a)$. We introduce endogenous amenities to approximate the evidence in Section 3.2, in which various amenity proxies respond to local population size.

Individuals of age $a \geq \underline{a}$ earn labor income, receive profits from land ownership, and pay taxes. We assume that agents do not have access to saving or borrowing technologies and

[8] For agents with age $a < \underline{a}$, we assume that they do not work and earn zero income. We also impose that they remain in their birth locations and do not migrate.

therefore fully consume their income each period. Therefore, the budget constraint for an individual is given by:

$$c_t^n(a) + R_t^n h_t^n(a) = y_t^n(a) \equiv (1-\kappa_t) w_t^n(a) + \widetilde{\pi}_t^n(a) + T_t \times 1[a \geq a^*] \tag{9}$$

The left-hand side of the equation is the expenditure on final goods and housing. The right-hand side denotes total disposable income $y_t^n(a)$, which comprises three components: labor income, land income, and pension transfers. Specifically, $w_t^n(a)$ is the labor compensation specific to location n, age a, and time t; κ_t is the labor income tax rate; $\widetilde{\pi}_t^n(a)$ is income from land ownership[9]; and T_t is the pension transfers received by the elderly ($a \geq a^*$).

After the production and consumption occur, agents decide on the living location for the next period to maximize the expected lifetime utility. The expected lifetime utility of an agent of age a at the beginning of period t in location n is given recursively by:

$$V_t^n(a) = \max_{c_t^n(a), h_t^n(a)} u_t^n\left(c_t^n(a), h_t^n(a), \chi_t^n(a)\right) + \mathbb{E}_t\left[\max_{\ell \in N}\left\{s_t^\ell(a)\beta V_{t+1}^\ell(a+1) - \tau_t^{n\ell}(a) + \nu\varepsilon_t^\ell(a)\right\}\right] \tag{10}$$

subject to the budget constraint in equation (9). $\tau_t^{n\ell}(a)$ denotes the migration costs in utility, which depend on the origin, destination, time, and age. β is the discount factor. Expectations, $\mathbb{E}_t$, are taken over the realizations of the idiosyncratic preference shocks, ε, assumed to follow an i.i.d. type-I extreme value distribution. The parameter ν governs the dispersion of these shocks. The survival rate $s_t^\ell(a)$ depends on the migration destination ℓ. The value of death is normalized to zero.

The type-I extreme value distribution of idiosyncratic shocks implies that the migration share of agents of age group a moving from origin n to destination i from period t to $t+1$ is given by:

$$\mu_t^{ni}(a) = \frac{\exp\left[s_t^i(a)\beta V_{t+1}^i(a+1) - \tau_t^{ni}(a)\right]^{1/\nu}}{\sum_\ell^N \exp\left[s_t^\ell(a)\beta V_{t+1}^\ell(a+1) - \tau_t^{n\ell}(a)\right]^{1/\nu}}, \tag{11}$$

and the expected lifetime utility for an agent of age group a in location n at time t is:

$$V_t^n(a) = u_t^n(a) + \nu \log \sum_\ell^N \exp\left[s_t^\ell(a)\beta V_{t+1}^\ell(a+1) - \tau_t^{n\ell}(a)\right]^{1/\nu}, \tag{12}$$

where $u_t^n(a)$ is the indirect flow utility derived from solving the static consumption problem.

[9] As described in detailed in Section 4.4, land in each location is owned equally by the residents of that location in each point in time.

As mentioned earlier, agents begin to make migration decisions starting from age group $\underline{a}$. For agents younger than this threshold ($a < \underline{a}$), we impose that they remain in their birth location: $\mu_t^{ni}(a) = 1$ for $n = i$ and $\mu_t^{ni}(a) = 0$ otherwise.

4.2 Population Transition

The population distribution across age groups and locations evolves based on the interplay between births, deaths, and migration decisions. Given the endogenous migration shares $\mu_t^{ni}(a)$ defined in equation (11), as well as the fertility rates $\varkappa_t^n(a)$ and survival rates $s_t^n(a)$, the law of motion for the population size of age group a in location n at period t, denoted by $L_t^n(a)$, is given by:

$$L_{t+1}^n(a) = \begin{cases} \sum_{a'} \varkappa_{t+1}^n(a') L_{t+1}^n(a') & \text{if } a = 0 \\ \sum_\ell s_t^\ell(a-1)\mu_t^{\ell n}(a-1)L_t^\ell(a-1) & \text{if } 0 < a < \bar{a} \\ \sum_\ell s_t^\ell(\bar{a}-1)\mu_t^{\ell n}(\bar{a}-1)L_t^\ell(\bar{a}-1) + \sum_\ell s_t^\ell(\bar{a})\mu_t^{\ell n}(\bar{a})L_t^\ell(\bar{a}) & \text{if } a = \bar{a} \end{cases}. \tag{13}$$

This accounting relationship corresponds to the "demographic balancing equation" in the demography literature and forms the basis of local population projections (see Smith et al., 2013). A key distinction in our framework is that migration flows, $\mu_t^{\ell n}(a)$, are endogenous and determined in equilibrium based on local economic conditions and migration costs.

4.3 Production

In each location, a perfectly competitive producer uses labor as the input to produce final goods. Labor is assumed to be perfectly substitutable across different age groups. The efficiency of one unit of labor depends on the age and location, denoted by $\varphi_t^n(a)$. We allow for agglomeration spillovers in labor productivity, such that the size of the local working-age population enhances efficiency, such that

$$\varphi_t^n(a) = \tilde{\varphi}_t^n(a)(L_t^{n,W})^{\gamma^p}, \tag{14}$$

where $\tilde{\varphi}_t^n(a)$ is an exogenous age-location-time specific productivity component, and γ^p captures the elasticity of agglomeration effects.

Production exhibits constant returns to scale and perfect substitutability across age groups, and is defined as:

$$Y_t^n = \sum_{a \geq \underline{a}} \varphi_t^n(a) L_t^n(a).$$

Given the perfect competition in local labor markets, as well as the tradable goods being

taken as numeraire, the equilibrium wage for an individual of age $a \geq \underline{a}$ in location n at period t is given by:

$$w_t^n(a) = \varphi_t^n(a), \quad \forall a \geq \underline{a}. \tag{15}$$

4.4 Housing

We assume that housing service is produced by a local competitive construction sector in each period using a Cobb-Douglas technology with land Z_t^n and effective labor $L_t^{n,H} = \sum_{a \geq \underline{a}} \varphi_t^n(a) L_t^{n,H}(a)$ as inputs:

$$H_t^n = \xi^n \left(L_t^{n,H}\right)^{\mu} \left(Z_t^n\right)^{1-\mu}, \tag{16}$$

where ξ^n denotes the location-specific housing sector productivity. Land is owned by households and supplied inelastically at a fixed value $\left\{\bar{Z}^n\right\}$.

The housing supply that solves the housing sector's profit maximization problem is:

$$R_t^n = \tilde{\xi}^n (H_t^n)^{\frac{1-\mu}{\mu}}, \tag{17}$$

where $\tilde{\xi}^n = (\xi^n)^{-\frac{1}{\mu}} \mu^{-1} \left(\bar{Z}^n\right)^{-\frac{1-\mu}{\mu}}$, and we assume that tradable goods are produced everywhere and hence the wage per efficiency unit of labor is equalized to tradable prices (numeraire). The housing supply depends on the level of land available and implies an inverse housing supply elasticity of $\frac{1-\mu}{\mu}$.

Equilibrium rent R_t^n is determined by the market-clearing condition in the local housing market. Aggregate housing demand from agents solving problem (10) is given by:

$$\tilde{H}_t^n = \theta \frac{\sum_{a > \underline{a}} y_t^n(a) L_t^n(a)}{R_t^n}, \tag{18}$$

where $y_t^n(a)$ is total income defined in (9). Substituting this into the housing supply equation (17), we obtain the equilibrium rent

$$R_t^n = \left(\tilde{\xi}^n\right)^{\mu} \left(\theta \sum_{a > \underline{a}} y_t^n(a) L_t^n(a)\right)^{1-\mu}. \tag{19}$$

Under perfect competition and the Cobb-Douglas housing production function, the total return to land equals a fixed share of total housing revenue, given by $(1-\mu) R_t^n H_t^n$. These returns are rebated in a lump sum to all local individuals above the minimum working age.

The resulting per capita land income, $\tilde{\pi}_t^n(a)$, is given by:

$$\tilde{\pi}_t^n(a) = \frac{\theta(1-\mu)\left(\sum_{a' \geq \underline{a}} y_t^n(a') L_t^n(a')\right)}{\sum_{a' \geq \underline{a}} L_t^n(a')} \times 1[a \geq \underline{a}]. \tag{20}$$

4.5 Government

The national government raises labor income tax, and uses it to finance pension transfers and local public services. The required level of public service is treated as a fixed cost necessary to sustain each local community, paid in units of tradable goods. Following the evidence in Section 3.2, we assume that the per capita fiscal cost g_t^n is a decreasing function of population size, given by

$$g_t^n = \zeta (L_t^n)^{-\gamma^g}, \text{ where } L_t^n \equiv \sum_{a \in A} L_t^n(a), \tag{21}$$

where ζ captures the productivity of public service provision. There is a negative relationship between fiscal cost per capita and local population size, governed by parameter γ^g. Hence, the fiscal cost of public service provision evolves endogenously with local demographic conditions. In contrast, we assume that the pension payments per recipient are uniform across locations.

The central government runs a balanced budget for each period, given by

$$\kappa_t \sum_n \sum_{a \geq \underline{a}} w_t^n(a) L_t^n(a) = \sum_n \sum_{a \geq a^*} T_t L_t^n(a) + \sum_n \sum_{a \in A} g_t^n L_t^n(a), \tag{22}$$

for each period t, where κ_t is the labor income tax rate, which can adjust over time to balance the government's budget.

4.6 Equilibrium

Denoting the location-, age-, time-specific variables by $x_t = \{x_t^n(a)\}_{a=0,n=1}^{\bar{a},N}$ and the location- and time-specific variables by $q_t = \{q_t^n\}_{n=1}^N$, given an initial allocation of agents of different ages across locations $\{L_0^n(a)\}$ and the sequence of fundamentals and taxes and transfer policies $\left\{\tilde{\varphi}_t, \tilde{\chi}_t, \tau_t, \varkappa_t, s_t, \tilde{\xi}, \zeta, T_t, \kappa_t\right\}_{t=0}^{\infty}$, a sequential competitive equilibrium is a sequence of allocations and prices $\{c_t, h_t, L_t, \mu_t, w_t, R_t, H_t, \tilde{\pi}_t, g_t\}_{t=0}^{\infty}$ that solves agents problem (10-11), satisfies low of motion of population (13), firms optimization conditions (15), housing market clearing conditions (17-18), land income (20), local public service cost (21), and government budget constraint (22).

5 Calibration

In this section, we calibrate our model to the Japanese economy. We use the 47 prefectures as the spatial units. We set 2015 as the initial year ($t = 0$) of the economy, and adopt five-year intervals as the model's time frequency. Accordingly, age is grouped into five-year intervals, with the oldest group representing those aged 70 and above, such that $\bar{a} = 14$. The legal working age in Japan is 15, which corresponds to $\underline{a} = 3$. Below, we discuss the calibration of structural parameters and location fundamentals.

5.1 Calibrated Structural Parameters

The calibrated structural parameters are summarized in Table 1.

Table 1: Calibrated Parameters and Exogenous Variables

Parameters	Description	Values / Sources
ν	shape parameter for migration preference shocks	0.4
β	discount factor	0.97^5
θ	consumption expenditure share of housing	0.33
μ	labor share in housing construction	0.7
γ^p	externality in productivity from working-age population	0.1
γ^a	externality in amenity from working-age population	0.08
$\{s_t^n(a)\}$	survival rates by age and year	official statistics (past and projection)
$\{\varkappa_t^n(a)\}$	fertility rates by age, year, locations	official statistics (past and projection)
T_t	pension payment per elderly population	aggregate payment equals 10% of total labor income in 2015
γ^g	elasticity of public service cost per capita	0.72
ζ	productivity of public service provision	aggregate payment equals 20% of total labor income in 2015

Note: Table 1 summarizes the calibrated parameters and exogenous inputs used in the quantitative analysis.

We set the shape parameter for migration preferences shocks, which proxies the inverse of migration elasticities, to $\nu = 0.4$. This value is consistent with the estimates from Suzuki

(2023), who estimates the corresponding migration elasticities across prefectures in Japan. The discount factor is set to $\beta = 0.97^5$, reflecting a standard annual rate applied to five-year periods. The housing expenditure share is set to $\theta = 0.33$, based on the average share of housing-related expenditures in Japan. We set the labor share in housing construction to $\mu = 0.7$, which is consistent with land share estimates in housing production from the literature, including Combes et al. (2021) for France and Tan et al. (2020) for China. This value implies a housing supply elasticity of $\mu/(1-\mu)$, or equivalently, an inverse elasticity of $(1-\mu)/\mu = 3/7$, as shown in equation (17).

We set the productivity and amenity spillover elasticities to $\gamma^p = 0.1$ and $\gamma^a = 0.08$, respectively. For productivity, we choose $\gamma^p = 0.1$ based on the broader agglomeration literature, which finds positive elasticities of productivity with respect to local economic density, as summarized by Melo et al. (2009), and on recent evidence for Japan in Hayakawa et al. (2021). For amenity externalities, we set $\gamma^a = 0.08$, which are in line with the estimates of Ahlfeldt et al. (2015). The positive amenity externality is consistent with our empirical findings that various amenity proxies are positively associated with population size, as we find in Section 3.2.

Fertility rates $\{\varkappa_t^n(a)\}$ and survival rates $\{s_t^n(a)\}$ before 2015 are calibrated based on age-specific fertility and deaths from the Vital Statistics, combined with population data from the Census. For the years after 2015, we use projected fertility and mortality rates published by the National Institute of Population and Social Security Research.[10] In the quantitative analysis, we assume that these rates can vary across age groups and over time, but do not depend on locations.[11]

We calibrate the pension benefits $\{T_t\}$ such that the total pension payment is 10% of the country's GDP, approximately the value observed in Japan in 2015.[12] Specifically, assuming

[10]The National Institute of Population and Social Security Research provides projections of fertility and mortality rates by age group through 2070 under three scenarios: high, medium, and low. We adopt the medium scenario for both fertility and mortality and assume that the projected 2070 levels remain constant thereafter. To ensure convergence to a steady state in the long run, which is necessary for simulating the model, we assume that each location reaches a replacement-level fertility rate starting in period $t = 200$, which corresponds to 1,000 years after the initial period.

[11]The survival rates in Japan have limited variation across prefectures (Appendix Figure B.4). Fertility rates vary across locations, with higher-income prefectures tending to have lower fertility rates (Appendix Figure B.5). However, as explained in the Appendix B.5, the spatial variation of newborns is primarily driven by the spatial distribution of reproductive age population, and the spatial variation of fertility rates plays a minimal role.

[12]According to Financial Statistics of Social Security in Japan (National Institute of Population and Social Security Research), total pension benefits have remained at around 10% of GDP since 2008.

the rate of productivity growth of 1% (as we assume in the next section), we set T_t to follow

$$T_t = \frac{10\% \times \sum_n^N \sum_{a \geq \underline{a}} w_{2015}^n(a) L_{2015}^n(a)}{\sum_n^N \sum_{a \geq a^*} L_{2015}^n(a)} \times (1 + 1\%)^{(t-2015)}, \tag{23}$$

for each t.

We set the negative elasticity of public service cost with respect to population to $\gamma^g = 0.72$, based on the estimation equation (21) without prefecture fixed effects but with initial fiscal spending per capita (in logs) as a control, to use cross-prefectural variation consistent with the spatial unit of our quantitative analysis. The positive value of γ^g captures the feature that the public service cost per capita goes up in a depopulating region, as we empirically find in Section 3.2. We set the public service productivity shifter ζ so that aggregate government spending accounts for 20% of aggregate labor income in 2015, as observed in Japan.

Finally, we set the labor income tax rate κ_t in each period to satisfy the government budget constraint in equation (22).

5.2 Inversion of Productivity, Amenity, and Migration Costs

We next describe how we calibrate the exogenous components of productivity, amenities, and migration costs. We recover these fundamentals in the initial period (2015) by inverting observed wages, migration flows, and population distributions in 2015.[13] For future projections, we hold all exogenous fundamentals fixed at their 2015 levels, except for productivity, which is assumed to grow at an annual rate of 1%, consistent with a typical value assumed in the context of Japan (Kitao, 2015; İmrohoroğlu et al., 2016).

Productivity $\{\tilde{\varphi}_t^n(a)\}$. From equation (15), labor productivity $\{\varphi_t^n(a)\}$ corresponds to their labor compensation per capita $w_t^n(a)$. We compute this value in the data as a product of location-, time-, and age-specific employment rate times annual average labor compensation per worker. We then recover the exogenous component of the productivity $\{\tilde{\varphi}_t^n(a)\}$ in 2015 using equation (14), such that

$$\tilde{\varphi}_t^n(a) = w_t^n(a)(L_t^{n,W})^{-\gamma^p} \tag{24}$$

Again, after 2015, we assume that $\tilde{\varphi}_t^n(a)$ grows uniformly at the rate of 1% annually.

[13] Our approach is analogous to the "dynamic hat algebra" method in Caliendo et al. (2019), but we explicitly invert fundamentals to accommodate time-varying fertility and survival rates.

Amenity $\{\tilde{\chi}_t^n(a)\}$ and Migration Costs $\{\tau_t^{ni}(a)\}$. We calibrate amenities and migration costs to rationalize the observed migration patterns. We first introduce a set of innocuous normalizations that do not affect the equilibrium allocation or normative implications. First, we normalize exogenous amenities $\tilde{\chi}_t^n(a)$ to one for all n, t, and a. Under our additive utility specification, an increase in amenities in period t is isomorphic to a reduction in migration costs in the previous period (up to a discounting adjustment), making the two isomorphic.[14] Second, we normalize the migration costs if staying in the same location to zero: $\tau_t^{nn}(a) = 0$ for all t, a, and n. As seen in equation (11), migration decisions depend only on relative value functions and migration costs, and hence the reference value is irrelevant for the location choices (i.e., it is isomorphic to an amenity shifter of the origin).

We assume that bilateral migration frictions remain constant after 2015. We back out the off-diagonal elements of migration frictions, $\{\tau^{ni}(a)\}$ for $n \neq i$, so that the model exactly replicates the observed migration patterns across space in 2015, $\{\mu_{2015}^{ni}(a)\}$. This is implemented using a recursive procedure. Additional details are provided in Appendix C.2.[15]

6 Future Projections

We now use our calibrated model to project the future patterns of the regional population and aging, starting from 2015. To elucidate the roles of migration and the spatial distribution of fertility in shaping regional patterns of population decline and aging, we conduct projections under three alternative model specifications. The first specification, labeled "Baseline," corresponds to the model described in Section 4. The second specification, "No migration," shuts down all interregional migration. In this case, population dynamics in each region are driven solely by the initial age distribution and natural population changes (births and deaths). The third specification, "Birth distribution in 2015," fixes the spatial distribution of births at its 2015 level. Under this specification, regional population dynamics are driven by the initial population distribution and migration patterns, but not by cross-regional differences in fertility arising from variation in the spatial distribution of the reproductive population.

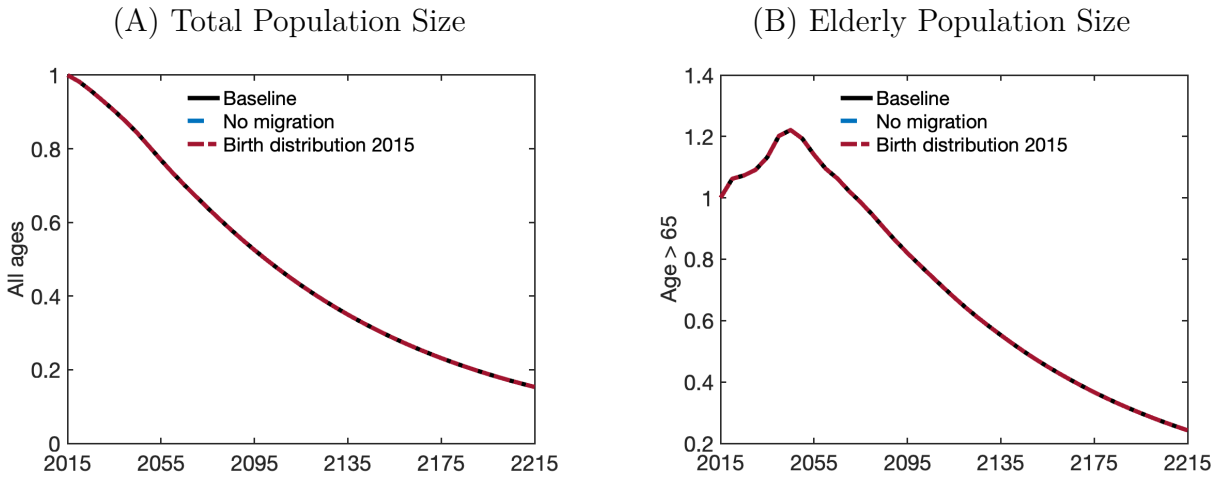
Figure 8 depicts the projected evolution of the population at the national level from 2015 to 2215. Panel (A) shows total population, while Panel (B) shows the elderly population (individuals aged 65 and above), with both series normalized to their 2015 levels. As discussed

[14] Similarly, we normalize the housing sector productivity parameter $\tilde{\xi}^n$ to one, as it also enters additively for each location.

[15] In Appendix C.3, we validate the model by reinitializing it in 1990. Specifically, we invert fundamentals using 1990 data, assume they remain fixed thereafter, and compare the model's predicted population changes to those observed through 2015. The model closely matches the observed population dynamics, providing supportive evidence for its validity.

in Section 2, Japan was already experiencing population decline in 2015. Under the projected fertility and survival rates, the total population falls to just under one-half of its 2015 level by 2100 and to about 15 percent by 2215. The elderly population initially rises, peaking at a little above 20 percent above its 2015 level around 2050 as existing working-age cohorts age into retirement. Thereafter, it declines and gradually converges toward the trend in total population. Note that, since we assume homogeneous fertility and survival rates across regions, the aggregate population distribution is unchanged across the three model specifications mentioned above ("Baseline," "No migration," and "Birth distribution in 2015").

Figure 8: Aggregate Future Population Transition



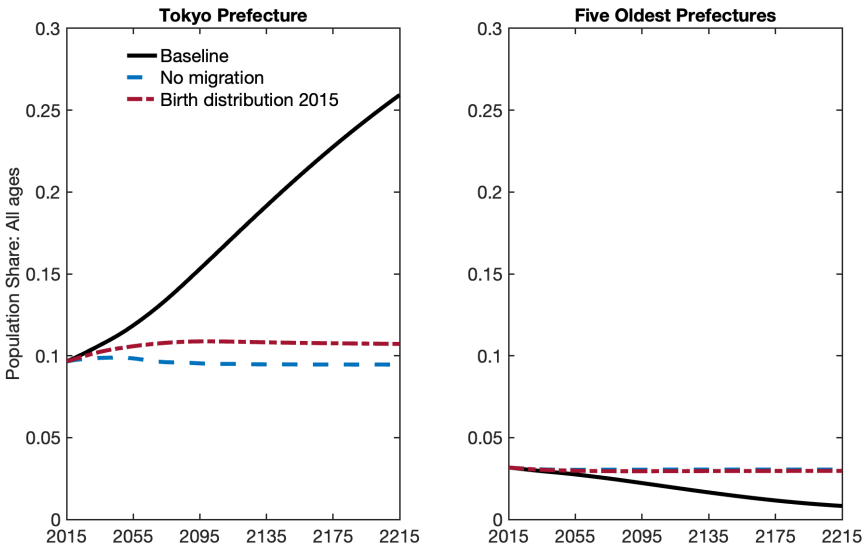
Note: Figure 8 reports model-implied aggregate total population and elderly population under the baseline, no-migration, and birth-distribution-in-2015 specifications. Each series is normalized to one in 2015. Because fertility and survival rates are assumed to be common across regions, the three specifications imply the same aggregate paths. Appendix Figure D.1 reports the same aggregate projection separately by age group.

Regional Depopulation and Aging In Figure 9, we show how these patterns of depopulation and aging occur differently across regions in Japan. Panel (A) shows the population share of Tokyo prefecture (left) and of the five oldest prefectures as of 2015 (right; contains Kochi, Shimane, Tokushima, Tottori, and Yamagata Prefectures), and Panel (B) shows the elderly population share. The three lines indicate the three alternative model specifications discussed above ("Baseline," "No migration," and "Birth distribution in 2015").

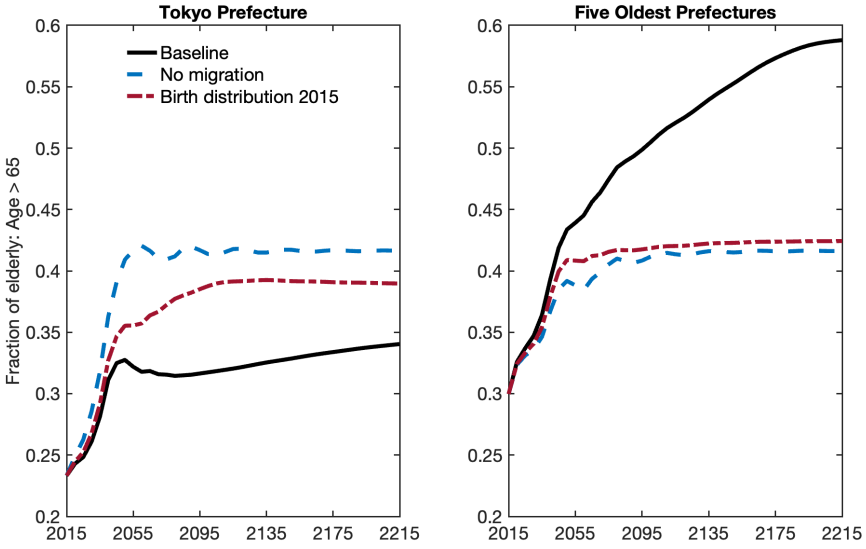
We first discuss population-share dynamics in Panel (A). Under the baseline specification ("Baseline"), the population share of Tokyo increases steadily over time. Starting from about 10 percent in 2015, it rises to roughly 15 percent by the end of the 21st century and to about 26 percent by 2215. In contrast, the combined population share of the five oldest

Figure 9: Projected Population Shares across Locations

(A) Population Share



(B) Elderly Population Share



Note: Figure 9 reports model-implied population shares for Tokyo prefecture and the five oldest prefectures as of 2015 under the baseline, no-migration, and birth-distribution-in-2015 specifications. Panel (A) shows total population shares, and Panel (B) shows elderly population shares. Appendix Figure D.2 presents the corresponding regional population-share paths separately by age group.

prefectures, which is about 3 percent in 2015, declines gradually to below 1 percent by the end of the horizon. These results indicate that the pattern of faster depopulation in rural areas documented in Section 3 is projected to persist, leading to increasing divergence, rather

than convergence, in regional population shares over the next two centuries.

This divergence is driven by both internal migration and the spatial distribution of births. When we shut down internal migration ("No migration"), the relative population shares of Tokyo and the five oldest prefectures remain close to their 2015 levels throughout the horizon. Similarly, when we fix the spatial distribution of births at its 2015 level ("Birth distribution in 2015"), Tokyo's share rises only modestly and the population share of the five oldest prefectures remains nearly flat.

Panel (B) shows that regional aging also diverges under the baseline specification. In Tokyo, the elderly share rises from about 23 percent in 2015 to roughly 32 percent by the 2050s, declines slightly thereafter, and then edges up to around 34 percent by 2215. In contrast, in the five oldest prefectures, the elderly share rises from about 30 percent in 2015 to roughly one-half by the end of the 21st century and to nearly 60 percent by 2215. By contrast, when migration is shut down or the spatial distribution of births is fixed, regional elderly shares remain much closer together, with Tokyo aging more rapidly and the five oldest prefectures aging more slowly than in the baseline.

The continued divergence in regional depopulation and aging patterns is consistent with a mechanism in which amenity and productivity spillovers generate a self-reinforcing feedback loop. In Tokyo, where the population of reproductive age is relatively large, population concentration persists over time. This concentration further enhances the region's attractiveness through agglomeration effects on productivity and amenities, which in turn induce additional in-migration, particularly of younger cohorts. The inflow of younger individuals raises local fertility, reinforcing concentration in relative population terms. This process creates a positive feedback cycle that drives sustained population concentration in Tokyo, while rural regions experience ongoing depopulation and aging.

To unpack those different mechanisms, we conduct a series of counterfactual exercises in which we shut down one mechanism at a time, holding the corresponding object fixed at its 2015 level. Specifically, we consider five alternative specifications relative to the baseline: fixing bilateral migration shares $\mu^{ni}(a)$ at their 2015 values ("Fixed migration"); fixing amenities $\chi^n(a)$/productivity $\varphi^n(a)$ at their 2015 levels ("No amenity/productivity spillover"); fixing housing rents R^n at their 2015 levels ("Fixed rent"); and fixing the per-capita fiscal cost of public services g^n at its 2015 level ("Fixed per-capita fiscal cost"). Comparing each counterfactual against the baseline isolates the contribution of the corresponding force to the projected divergence in regional depopulation and aging. Appendix Figure D.5 reports the implied population shares and elderly shares for Tokyo prefecture and the five oldest prefectures.

Several channels, when shut down, attenuate the divergence. Fixing the migration matrix

at its 2015 level substantially dampens the concentration of population in Tokyo: rather than rising toward roughly 26 percent by 2215 as in the baseline, Tokyo's share increases only modestly to about 14 percent, while the share of the five oldest prefectures remains well above its baseline path. Removing either the amenity or the productivity spillover operates in the same direction, muting Tokyo's rise and slowing the decline of the oldest prefectures, which confirms that the self-reinforcing feedback between population size and local productivity and amenities is a key amplifier of regional divergence. By contrast, fixing the per-capita fiscal cost of public services leaves the projected paths essentially unchanged, indicating that the endogeneity of public service costs, while important for the aggregate fiscal implications discussed later, plays only a minor role in shaping the spatial distribution of population itself. The most dramatic departure arises when housing rents are held fixed: Tokyo absorbs almost all the population within a few decades while the oldest prefectures collapse to near zero, highlighting the central role of housing as a congestion force that, in the baseline, partially offsets the agglomeration gains and restrains population concentration.

These channels are also visible in the projected paths of regional aging. Fixing migration or removing either spillover keeps the elderly shares of Tokyo and the five oldest prefectures much closer together than in the baseline: the oldest prefectures age less, reaching an elderly share of about 45 percent rather than nearly 60 percent, while Tokyo ages relatively more. This is consistent with the interpretation that the out-migration of younger cohorts drives the divergence in age structure. When housing rents are fixed, because the oldest prefectures lose nearly all of their working-age population, their elderly share spikes toward 100 percent around 2055 before declining as the remaining elderly population shrinks. Taken together, these decompositions indicate that endogenous migration and agglomeration spillovers are the primary forces driving regional divergence in both depopulation and aging, that housing rents act as the key counteracting dispersion force.

Flow Utility and Its Inequality To assess this mechanism and its implications for inequality, Figure 10 reports the flow utility for the working-age population (Panel A) and the elderly (Panel B). The flow utility takes into account the consumption of final good and housing, as well as endogenous amenity spillover.[16] In both panels, we normalize flow utility in Tokyo in 2015 to zero for each age group. The three lines correspond to the alternative model specifications discussed above: "Baseline," "No migration," and "Birth distribution in

[16] Specifically, unlike equation (7), Figure 10 plots $(1-\theta)\ln c_t^n(a) + \theta \ln h_t^n(a) + \gamma^a \ln L_t^{n,W}$. The exogenous amenity term $\ln \widetilde{\chi}_t^n(a)$ cannot be separately identified from migration costs, as discussed in Appendix C.2. Consequently, when comparing locations at a given calendar date, our flow utility measure may either understate or overstate the true utility gap between locations due to unobserved differences in exogenous amenities across locations. However, to the extent that such a gap exists, it remains constant along the transition path.

2015."

Under the baseline specification, Tokyo's flow utility increases more rapidly than that of the five oldest prefectures (comparing the figures in the left and the right). This divergence is observed across all age groups, but is much more pronounced for the working-age population (Panel A) than for the elderly (Panel B), reflecting the fact that elderly individuals rely more heavily on pension income, which is location-independent. In contrast, when internal migration is shut down ("No migration") or when the spatial distribution of births is fixed at its 2015 level ("Birth distribution in 2015"), flow utility evolves in a roughly parallel manner across regions. These patterns are again consistent with an interpretation that the migration and fertility dynamics create a positive feedback loop in Tokyo prefecture, amplifying wage and amenity gains there while attenuating them in other regions.[17]

Aggregate Production and Fiscal Cost of Local Public Service Provision Finally, we examine the implications for aggregate outcomes. Panel (A) of Figure 11 reports labor income per capita, and Panel (B) reports fiscal spending per capita, with both series normalized to one in 2015. Under the baseline scenario, labor income per capita continues to rise substantially: it reaches about 1.8 times its 2015 level by 2100 and slightly above five times its 2015 level by 2215. In contrast, when internal migration is shut down or when the spatial distribution of births is fixed, growth is slower, reaching only about 4.6 times the 2015 level by 2215. These differences reflect productivity heterogeneity across locations. Because Tokyo has higher productivity, population reallocation toward more productive regions raises aggregate income through a composition effect.

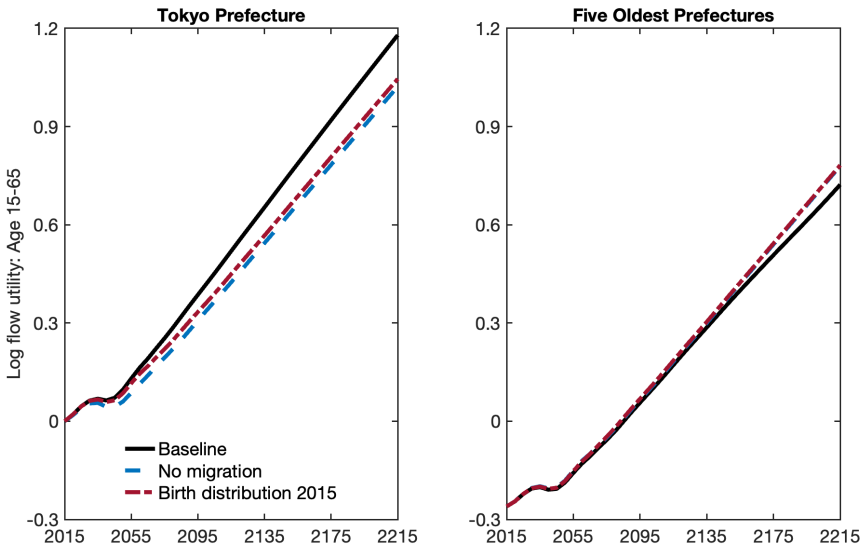
Panel (B) shows that population concentration also improves aggregate efficiency by reducing the per-capita cost of providing local public services. In the baseline scenario, fiscal spending per capita increases to about 1.7 times its 2015 level by 2100 and to nearly 3.3 times its 2015 level by 2215, reflecting increasing returns in local public service provision (see equation (21)). By contrast, under "No migration" or "Birth distribution in 2015," fiscal spending grows more rapidly, reaching roughly 3.8 times its 2015 level by 2215. These patterns arise because densely populated regions, such as Tokyo, can provide public services at lower per-capita cost. As a result, population concentration reduces the aggregate fiscal burden of local public service provision.

Figure 12 shows the evolution of labor income tax κ_t. Under "No migration" or "Birth distribution in 2015", lower income per-capita and higher fiscal spending per capita translate into higher income tax rate needed to finance the pension system and public services. By 2215, tax rate would be 6 percent higher compared to the baseline economy.

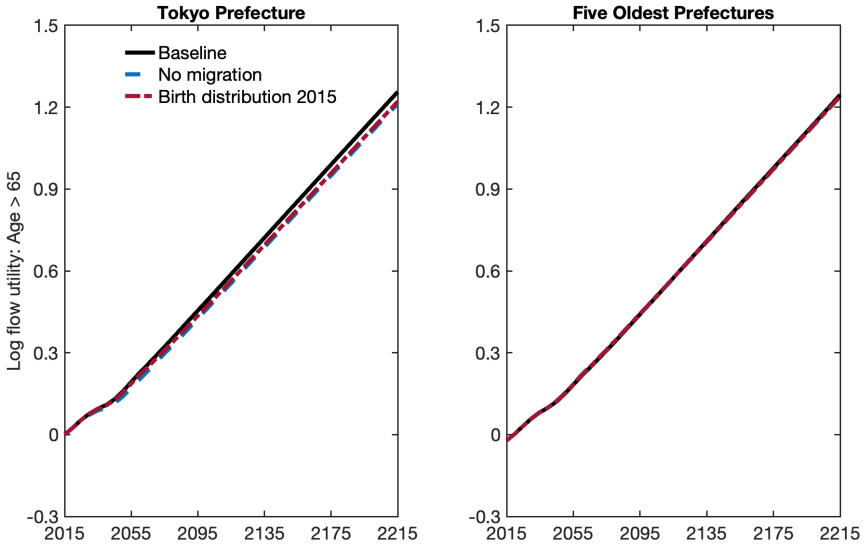
[17]Appendix Figure D.3 reports the corresponding regional paths of wages and shows similar patterns.

Figure 10: Flow Utility, By Location

(A) Working-Age (Age 15-65)



(B) Elderly (Over 65)

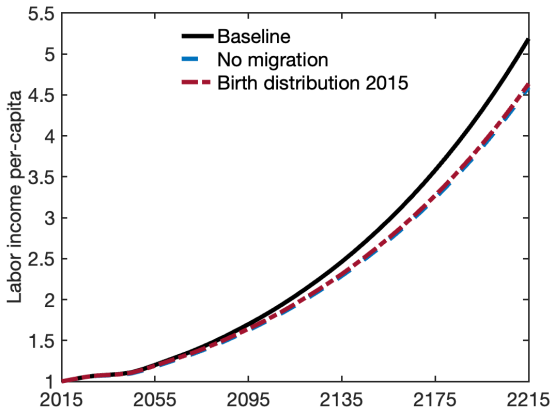


Note: Figure 10 reports model-implied flow utility for Tokyo prefecture and the five oldest prefectures as of 2015 under the baseline, no-migration, and birth-distribution-in-2015 specifications. In each panel, values are normalized so that Tokyo in 2015 equals zero for the corresponding age group. Appendix Figure D.4 reports the same comparison separately for finer age groups. Appendix Figure D.3 reports the corresponding regional paths of wages and housing rents.

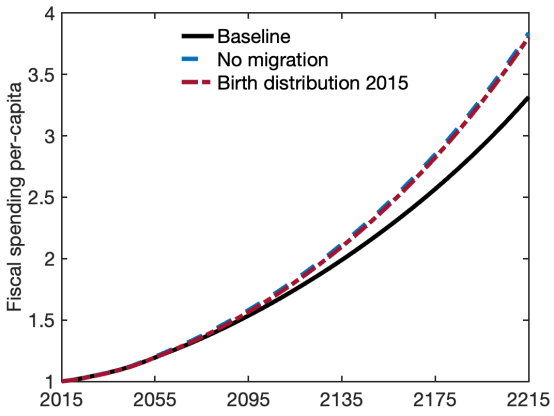
Robustness: CES Housing Production Our baseline assumes a Cobb-Douglas housing production technology, which implies a constant land share and hence a constant housing

Figure 11: Projected Aggregate Income and Fiscal Spending per Capita

(A) Aggregate Income per Capita

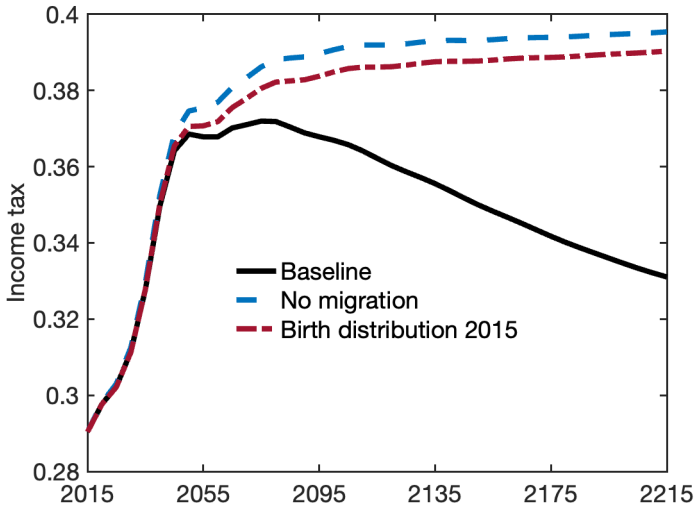


(B) Fiscal Spending per Capita



Note: Figure 11 reports model-implied aggregate labor income per capita and fiscal spending per capita under the baseline, no-migration, and birth-distribution-in-2015 specifications. Each series is normalized to one in 2015.

Figure 12: Projected Labor Income Tax Rate



Note: Figure 12 reports the model-implied labor income tax rate κ_t from 2015 onward under the baseline, no-migration, and birth-distribution-in-2015 specifications. The tax rate finances pensions and local public services in the model economy.

supply elasticity across locations and over time. This assumption is convenient but restrictive: it forces the responsiveness of rents to local population to be invariant to how scarce or abundant land has become. To assess the sensitivity of our results to this assumption, we

re-calibrate the model replacing equation (16) with a constant elasticity of substitution (CES) technology between effective labor and land. We set the elasticity of substitution to 0.9 following Combes et al. (2021), so that the two inputs are complements.[18] Under this specification, as population declines and land becomes increasingly abundant relative to labor, land share in the housing production drops over time. Appendix Figures D.6 through D.10 compare the resulting future projections to the baseline.

The declining land share over time weakens the congestion force that helps retain population in shrinking regions in the baseline. Tokyo's population share rises to roughly 32 percent by 2215 under CES housing, compared with about 26 percent in the baseline, while the combined share of the five oldest prefectures falls below its baseline path. The amplified reallocation of the working-age population away from the periphery further accelerates aging there: the elderly share in the five oldest prefectures rises far above the baseline, peaking near 95 percent. The intensified divergence in population also widens the long-run gap in regional wages and flow utility, as the loss of working-age population in the oldest prefectures erodes the local agglomeration benefits to productivity and amenities. In terms of aggregate fiscal implications, as population concentrates more heavily in high-productivity Tokyo, aggregate labor income per capita rises slightly above the baseline, while aggregate fiscal spending per capita falls below it, reflecting the lower per-capita cost of providing public services in more densely populated regions. The resulting income tax to finance the pension system and fiscal spending becomes lower.

Overall, allowing for an endogenous housing supply elasticity strengthens our central finding: the forces driving regional divergence in depopulation and aging – and the associated trade-off between aggregate efficiency and spatial inequality – are robust to and amplified by a more flexible and realistic specification of housing production.

Taking Stock Our model simulations suggest that the divergent regional trends in population decline and aging are likely to persist over the next 200 years. These dynamics are driven by both internal migration and the spatial distribution of births, and are further amplified by agglomeration spillovers and their feedback effects. Tokyo prefecture—where a large share of the population is projected to concentrate—experiences a relative increase in flow utility compared with aging and depopulating regions, thereby exacerbating regional inequality.

At the same time, this spatial concentration yields aggregate efficiency gains: it raises overall productivity and reduces the per capita cost of providing local public services by

[18] Specifically, housing production is given by $H_t^n = \xi^n \left(\alpha^n \left(L_t^{n,H} \right)^{\frac{\sigma-1}{\sigma}} + (1-\alpha^n) \left(Z_t^n \right)^{\frac{\sigma-1}{\sigma}} \right)^{\frac{\sigma}{\sigma-1}}$. We set $\sigma = 0.9$, and calibrate α^n such that labor share in the housing production in 2015 is 0.7 across all the prefectures as in the baseline.

shifting population away from less productive and more costly regions. Taken together, these results highlight a fundamental efficiency–equity trade-off facing policymakers in addressing regional disparities in depopulation and aging, a topic we explore in the next section.

7 Place-Based Transfers

In this section, we examine how resident-based place policies affect projected regional depopulation and aging. The exercise is motivated by Japan's *Chiho Sosei* regional revitalization agenda, which began in 2014 and remains a central policy framework for addressing local population decline, reducing excessive concentration in the Tokyo area, and encouraging population flows toward non-metropolitan regions (Cabinet Office, Government of Japan, 2024). These policies include national and local programs that provide financial support for migration, settlement, employment, entrepreneurship, housing, and childrearing in depopulating and aging regions.

Related policies are also prominent in Europe. The European Commission's Long-Term Vision for Rural Areas includes a Rural Pact and a Rural Action Plan, aiming to make rural regions stronger, more connected, resilient, and prosperous by 2040 (European Commission, 2021). Spain's 2021 demographic challenge strategy mobilizes over €10 billion across 130 measures to address depopulation and territorial imbalance (*Plan de 130 medidas frente al reto demográfico*, Government of Spain, 2021). Italy's National Strategy for Inner Areas targets on territories affected by demographic decline, combining improved access to essential services with place-based development investments (OpenCoesione, 2026).

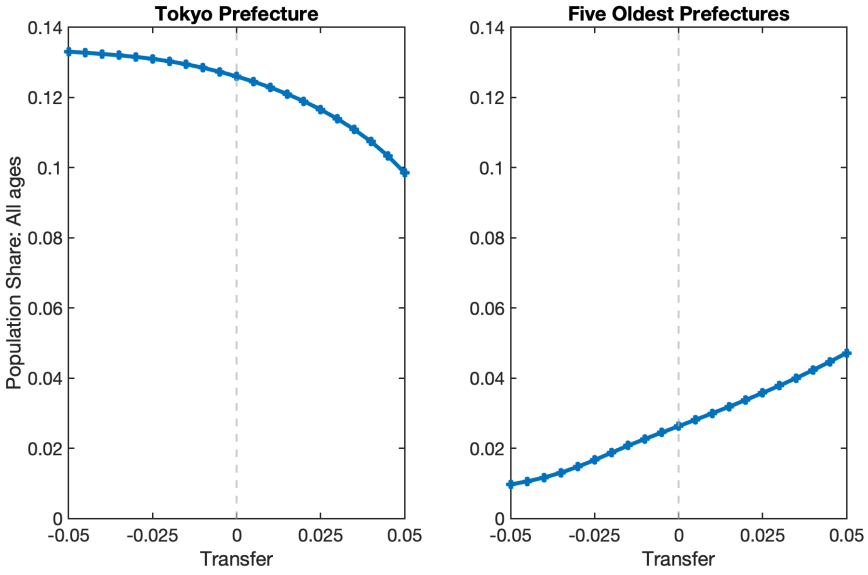
To capture the central economic forces behind such policies, we analyze the implications of monetary transfers to residents of the five oldest prefectures as of 2015, financed by higher labor income taxes in Tokyo prefecture. We do not interpret the exercise as a literal evaluation of any specific program. Rather, it provides a benchmark for quantifying how transfers conditional on residence affect long-run population dynamics, aging, flow utility across regions and cohorts, aggregate productivity, and fiscal costs.

Figure 13 illustrates the effects of these transfers on population shares (Panel A) and the share of the elderly (Panel B) for Tokyo prefecture (left panels) and the five oldest prefectures (right panels). In each panel, the x-axis denotes the transfer rate to the five oldest prefectures relative to the sum of their labor and pension income. For instance, a value of 0.01 implies that residents in these prefectures receive transfers equal to 1 percent of their labor and pension income combined, financed by a proportional labor income tax on residents of Tokyo, and a value of 0 corresponds to the baseline equilibrium without place-based transfers. We assume that the transfers are implemented for 100 years starting from 2015. The figure

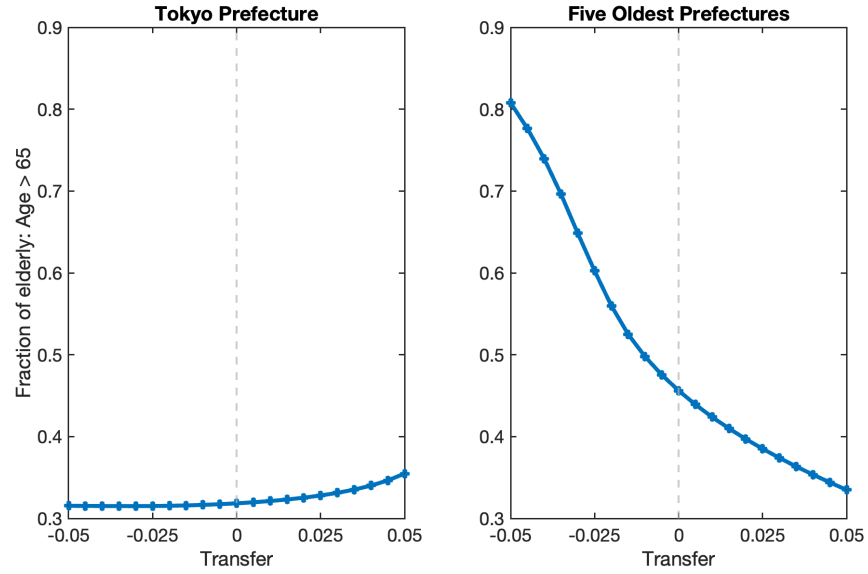
reports the implied outcomes in 2065.[19]

Figure 13: The Effect of Transfers to Five Oldest Prefectures: Population in 2065

(A) Population Share



(B) Elderly Population Share



Note: Figure 13 reports 2065 outcomes as a function of the transfer rate to the five oldest prefectures relative to their labor and pension income combined, financed by a proportional labor-income tax on Tokyo residents. Panel (A) shows total population shares, and Panel (B) shows elderly population shares. A transfer rate of zero corresponds to the baseline equilibrium without place-based transfers.

[19]In Appendix Figure D.11, we compare the impacts of transfers for different durations, from 10 years to 100 years. Naturally, the impacts of the policy increase in the assumed durations.

In Panel (A), we find that place-based transfers have a substantial impact on population distribution. In the baseline scenario without transfers, Tokyo prefecture is projected to account for about 12.5 percent of the population in 2065, while the five oldest prefectures together account for roughly 2.5 to 3 percent. Increasing transfers to the five oldest prefectures by 5 percent of their income reduces Tokyo's population share to 10 percent and raises that of the oldest prefectures to about 4.5 to 5 percent. Thus, even relatively modest transfer rates have meaningful effects on future population shares.

In Panel (B), we present the corresponding effects on population aging. The impacts in the five oldest prefectures are particularly striking. In the baseline scenario, the elderly share in these regions is projected to reach about 45 percent in 2065. Introducing transfers equal to 5 percent of income reduces this share to roughly one-third. In contrast, imposing a tax of the same magnitude increases the elderly share to about 80 percent. These patterns reflect differential migration responses across age groups: younger individuals are more responsive to location-specific incentives because their income is tied to local labor markets, whereas the elderly receive pensions that are location-invariant. Moreover, younger cohorts have longer planning horizons, making them more sensitive to persistent spatial differences in taxes and transfers.

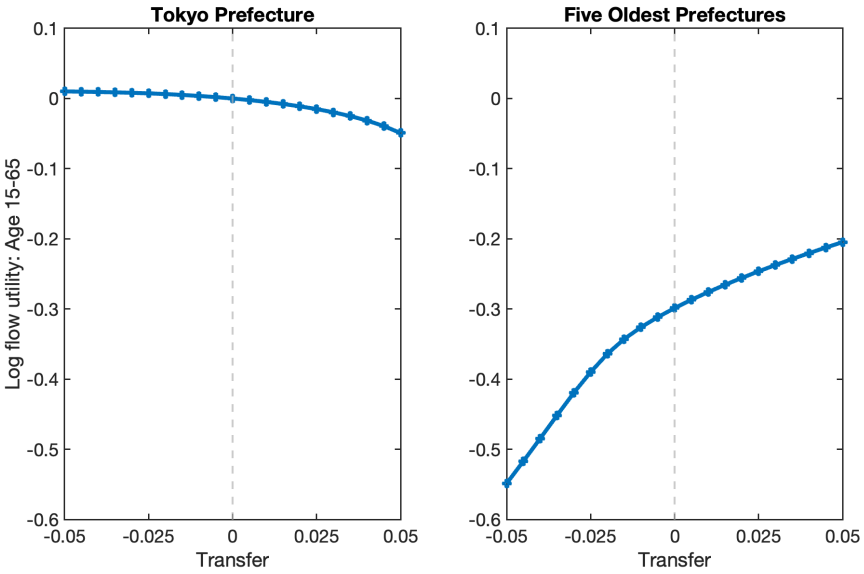
In Figure 14, we report the flow utility for the working-age population (Panel A) and the elderly (Panel B). In both panels, flow utility is normalized to zero for Tokyo prefecture in the absence of place-based transfers. As discussed in Section 6, without such transfers, the working-age population in the five oldest prefectures experiences substantially lower flow utility, by about 0.3 log points (Panel A). A similar but much smaller gap exists for the elderly, amounting to roughly 0.01 log points (Panel B).

Introducing transfers equal to 5 percent of income to the five oldest prefectures increases the flow utility of the working-age population in those regions by about 0.1 log points, while reducing that of Tokyo by about 0.05 log points. These results indicate that place-based transfers meaningfully reduce spatial inequality in flow utility. Notably, the gain in the five oldest prefectures exceeds the direct transfer amount, reflecting endogenous population responses and the resulting improvements in local productivity and amenities. In contrast, the decline in Tokyo's flow utility is more modest, largely because of its larger population base, which implies that the tax rate required to finance the transfers is below 5 percent. Panel (B) shows a similar pattern for the elderly. However, the baseline regional disparity is smaller, as their primary income source, pensions, is location-invariant. As a result, with place-based transfers, the elderly in the five oldest prefectures may even attain higher flow utility than their counterparts in Tokyo.

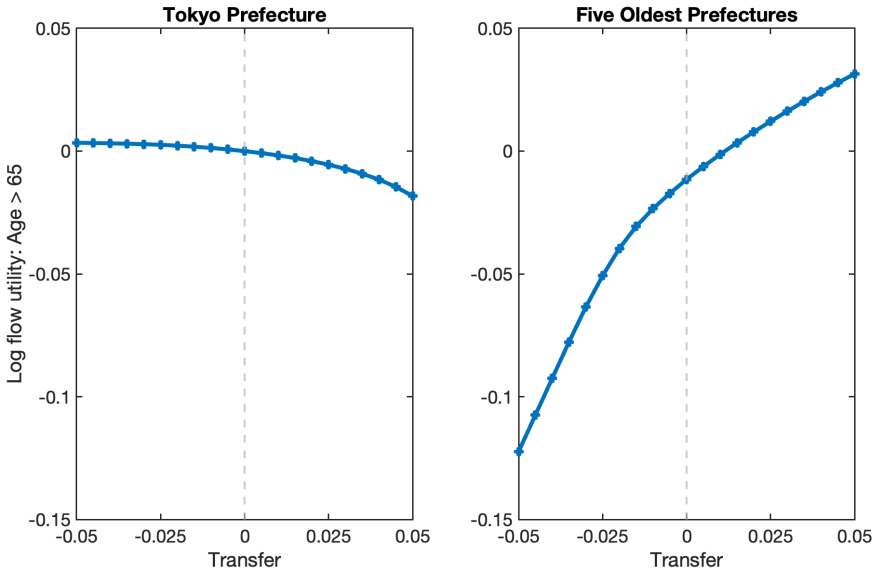
In Figure 15, we present the effects on aggregate income per capita (Panel A) and fiscal

Figure 14: The Effect of Transfers to Five Oldest Prefectures: Flow Utility in 2065

(A) Working-Age (Age 15-65)



(B) Elderly (Over 65)



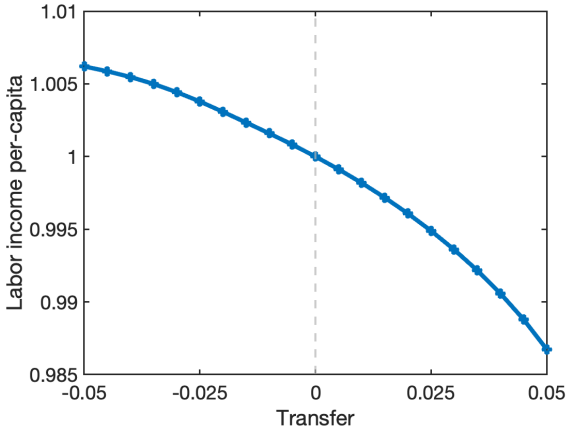
Note: Figure 14 reports the flow utility in 2065 as a function of the transfer rate to the five oldest prefectures relative to their labor and pension income combined, financed by a proportional labor-income tax on Tokyo residents. In each panel, values are normalized to zero for Tokyo in the absence of place-based transfers.

spending per capita (Panel B). In both panels, values are normalized to one in the absence of place-based transfers. Panel (A) shows that introducing transfers equal to 5 percent of income to the five oldest prefectures reduces aggregate income per capita by about 1.3 percent. Panel (B) indicates that aggregate fiscal spending per capita increases by 0.7 percent under

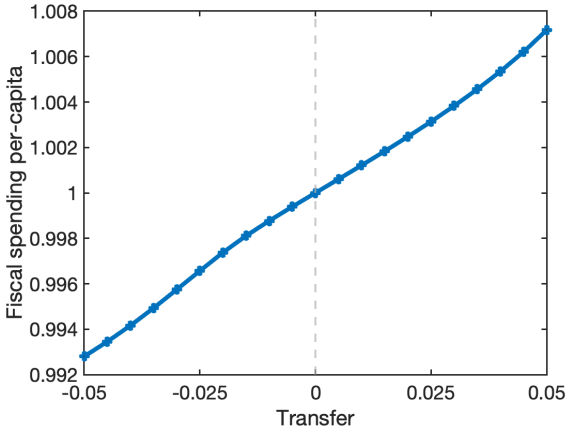
the same policy. These patterns are consistent with an interpretation in which place-based transfers reallocate population toward less productive regions with higher costs of providing local public services, thereby generating an aggregate efficiency loss.

Figure 15: The Effect of Transfers to Five Oldest Prefectures: Aggregate Income and Fiscal Spending per Capita in 2065

(A) Aggregate Income per Capita



(B) Fiscal Spending per Capita



Note: Figure 15 reports aggregate labor income per capita and fiscal spending per capita in 2065 as a function of the transfer rate to the five oldest prefectures relative to their labor and pension income combined, financed by a proportional labor-income tax on Tokyo residents. Both series are normalized to one in the absence of place-based transfers.

Overall, these results highlight a clear trade-off associated with place-based transfers aimed at mitigating depopulation and aging. While such policies benefit residents in declining and aging regions through redistribution, they also entail aggregate efficiency losses by reallocating population toward less productive locations with higher costs of public service provision. Our framework allows us to simulate the dynamic effects of these policies on future regional patterns of depopulation and aging, and to quantify this efficiency–equity trade-off.

8 Conclusions

In this paper, we study the process of depopulation and population aging across regions. Using spatially disaggregated data from Japan over the past four decades, we document that rural areas have experienced substantially faster depopulation and aging than urban areas, driven by low fertility and persistent outmigration of younger cohorts. Regions undergoing these trends face declining availability of local services and rising per-capita public service costs.

We then develop a dynamic spatial equilibrium model with endogenous fertility and migration. After calibrating the model to Japanese data, we use it to project future regional patterns of depopulation and aging. The model predicts that these processes will continue to diverge across regions, driven by the migration of younger cohorts and the associated fertility dynamics, and amplified by agglomeration forces.

Finally, we examine the role of place-based transfers in mitigating projected regional disparities in population decline and aging. We find that such policies involve a tight efficiency–equity trade-off: while they benefit residents in declining and aging regions through redistribution, they also generate aggregate efficiency losses by reallocating population toward less productive locations with higher public service costs.

An important remaining question concerns the optimal design of place-based policies to address regionally uneven depopulation and aging. Addressing this issue requires specifying a social welfare function that governs the trade-off between aggregate efficiency and spatial inequality, as in Donald et al. (2025) within a dynamic spatial general equilibrium framework. Another important set of policy questions concerns the role of infrastructure policies in response to regional depopulation and aging. We leave these analyses for future work.

References

Acemoglu, Daron and Pascual Restrepo, "Demographics and automation," *The Review of Economic Studies*, 2022, *89* (1), 1–44.

Ahlfeldt, Gabriel M., Ismir Mulalic, Caterina Soto-Vieira, and Daniel M. Sturm, "The Geography of Life: Evidence from Copenhagen," 2025. Working paper.

Ahlfeldt, Gabriel, Redding Stephen J., Sturm Daniel, and Wolf Nikolaus, "The Economics of Density: Evidence From the Berlin Wall," *Econometrica*, 2015, *83* (6), 2127–2189.

Ales, Laurence and Christopher Sleet, "Optimal Taxation of Income-Generating Choice," *Econometrica*, 2022, *90* (5), 2397–2436.

Allen, Treb and Costas Arkolakis, "Trade and the Topography of the Spatial Economy," *The Quarterly Journal of Economics*, 2014, *129* (3), 1085–1140.

Arkolakis, Costas, Jun Hee Kwak, Jaemin Woo, and Hyunjoo Yang, "Revisiting the Fertility Puzzle: A Dynamic Spatial Equilibrium Approach," 2026. Working paper.

Auclert, Adrien, Hannes Malmberg, Frédéric Martenet, and Matthew Rognlie, "Demographics, wealth, and global imbalances in the twenty-first century," 2025.

Bazzi, Samuel, Andreas Ferrara, Martin Fiszbein, Thomas Pearson, and Patrick A Testa, "The Other Great Migration: Southern Whites and the New Right," *The Quarterly Journal of Economics*, 2023, *138* (3), 1577–1647.

Berry, Christopher R. and Edward L. Glaeser, "The Divergence of Human Capital Levels Across Cities," September 2005, (11617).

Boustan, Leah Platt, "Was postwar suburbanization "white flight"? Evidence from the black migration," *The Quarterly Journal of Economics*, 2010, *125* (1), 417–443.

Braun, R Anton and Douglas H Joines, "The implications of a graying Japan for government policy," *Journal of Economic Dynamics and Control*, 2015, *57*, 1–23.

Cabinet Office, Government of Japan, "Chiho Sosei 10-nen no Torikumi to Kongo no Suishin Hoko [Ten Years of Regional Revitalization and Future Directions]," https://www.chisou.go.jp/sousei/meeting/chisoudecade/index.html 2024. Accessed June 9, 2026.

Caliendo, Lorenzo, Maximiliano Dvorkin, and Fernando Parro, "Trade and labor market dynamics: General equilibrium analysis of the china trade shock," *Econometrica*, 2019, *87* (3), 741–835.

Combes, Pierre-Philippe, Gilles Duranton, and Laurent Gobillon, "The production function for housing: Evidence from France," *Journal of Political Economy*, 2021, *129* (10), 2766–2816.

_ , _ , _ , Diego Puga, and Sébastien Roux, "The Productivity Advantages of Large Cities: Distinguishing Agglomeration from Firm Selection," *Econometrica*, 2012, *80* (6), 2543–2594.

Davis, Morris and Jesse Gregory, "Place-Based Redistribution in Location Choice Models," Working Paper 29045, National Bureau of Economic Research 2021.

Derenoncourt, Ellora, "Can you move to opportunity? Evidence from the Great Migration," *American Economic Review*, 2022, *112* (2), 369–408.

Diamond, Rebecca, "The Determinants and Welfare Implications of US Workers' Diverging Location Choices by Skill: 1980-2000," *American Economic Review*, March 2016, *106* (3), 479–524.

Donald, Eric, Masao Fukui, and Yuhei Miyauchi, "Optimal Dynamic Spatial Policy," Working Paper 34290, National Bureau of Economic Research 2025.

_ , _ , and _ , "Unpacking Aggregate Welfare in a Spatial Economy," *Review of Economic Studies (forthcoming)*, 2026.

Engbom, Niklas, "Firm and worker dynamics in an aging labor market," Technical Report, Federal Reserve Bank of Minneapolis Minneapolis, MN 2019.

European Commission, "A long-term Vision for the EU's Rural Areas: Towards Stronger, Connected, Resilient and Prosperous Rural Areas by 2040," 2021.

Fajgelbaum, Pablo and Cecile Gaubert, "Optimal Spatial Policies, Geography, and Sorting," *The Quarterly Journal of Economics*, 2020, *135* (2), 959–1036.

Gaigné, Carl and Jacques-François Thisse, "Aging nations and the future of cities," *Journal of Regional Science*, 2009, *49* (4), 663–688.

Gaubert, Cecile, Patrick Kline, Damian Vergara, and Danny Yagan, "Place-Based Redistribution," Working Paper 28337, National Bureau of Economic Research 2021.

Giannone, Elisa, "Skilled-biased technical change and regional convergence," 2021.

_ , **Qi Li, Nuno Paixao, and Xinle Pang**, "Unpacking Moving," Technical Report, Working Paper 2020.

Government of Spain, "Plan of Measures to Combat the Demographic Challenge," 2021.

Hayakawa, Kazunobu, Hans R. A. Koster, Takatoshi Tabuchi, and Jacques-Francois Thisse, "High-speed Rail and the Spatial Distribution of Economic Activity: Evidence from Japan's Shinkansen," Discussion Paper 21-E-003, Research Institute of Economy, Trade and Industry 2021.

Hopenhayn, Hugo, Julian Neira, and Rish Singhania, "From Population Growth to Firm," 2021.

Hsieh, Chang-Tai and Enrico Moretti, "Why Do Cities Matter? Local Growth and Aggregate Growth," May 2015, (21154).

İmrohoroğlu, Selahattin, Sagiri Kitao, and Tomoaki Yamada, "Achieving fiscal balance in Japan," *International Economic Review*, 2016, *57* (1), 117–154.

Jones, Charles I, "The end of economic growth? Unintended consequences of a declining population," *American Economic Review*, 2022, *112* (11), 3489–3527.

Karahan, Fatih, Benjamin Pugsley, and Ayşegül Şahin, "Demographic origins of the startup deficit," Technical Report, National Bureau of Economic Research 2019.

Kitao, Sagiri, "Fiscal cost of demographic transition in Japan," *Journal of Economic Dynamics and Control*, 2015, *54*, 37–58.

_ **and Minamo Mikoshiba**, "Females, the elderly, and also males: Demographic aging and macroeconomy in Japan," *Journal of the Japanese and International Economies*, 2020, *56*, 101064.

Komissarova, Kristina, "Location Choices over the Life Cycle: The Role of Relocation for Retirement," 2022.

Kondo, Keisuke, "Municipality-level panel data and municipal mergers in Japan," *RIETI Technical Paper*, 2019.

Maroto, Marco A. Badilla, Benjamin Faber, Antoine B. Levy, and Mathilde Muñoz, "Senior Migration, Local Economic Development and Spatial Concentration," Working Paper 34725, National Bureau of Economic Research 2026.

Masuda, Hiroya, "Chiho Shometsu: Tokyo ikkyyoku shuchu ga maneku jinko kyugen [Extinction of Rural Municipalities: Rapid population decline in rural Japan caused by unipolar centralization in Tokyo] (in Japanese)," 2014.

Melo, Patricia C., Daniel J. Graham, and Robert B. Noland, "A meta-analysis of estimates of urban agglomeration economies," *Regional Science and Urban Economics*, 2009, *39* (3), 332–342.

Mongey, Simon and Michael E Waugh, "Discrete choice, complete markets, and equilibrium," Working Paper 32135, National Bureau of Economic Research 2024.

Moreno-Maldonado, Ana and Clara Santamaria, "Delayed Childbearing and Urban Revival," 2022.

Moretti, Enrico, *The New Geography of Jobs*, Houghton Mifflin Harcourt, 2012.

Mori, Tomoya and Daisuke Murakami, "Sustainability of cities under declining population and decreasing distance frictions: The case of Japan," *arXiv preprint arXiv:2505.08333*, 2025.

OpenCoesione, "National Strategy for Internal Areas," 2026. Accessed June 8, 2026.

Redding, Stephen and Esteban Rossi-Hansberg, "Quantitative Spatial Economics," *Annual Review of Economics*, 2017, *9* (1), 21–58.

Smith, Stanley K, Jeff Tayman, and David A Swanson, "State and local population projections: Methodology and analysis," 2006.

_ , _ , and _ , *A practitioner's guide to state and local population projections*, Springer, 2013.

Suzuki, Yuta, "Local Shocks and Regional Dynamics in an Aging Economy," 2023. Working paper.

Takahashi, Takaaki, "On the economic geography of an aging society," *Regional Science and Urban Economics*, 2022, p. 103798.

Tan, Ya, Zhi Wang, and Qinghua Zhang, "Land-use regulation and the intensive margin of housing supply," *Journal of Urban Economics*, 2020, *115*, 103199.

United Nations, "World Population Prospects 2019," 2019.

Wrona, Jens, "Border effects without borders: What divides Japan's internal trade?," *International Economic Review*, 2018, *59* (3), 1209–1262.

Online Appendix for "Living in a Ghost Town: The Geography of Depopulation and Aging"

June 2026

A Data Sources **2**

B Appendix for Reduced-Form Facts **4**
B.1 Aggregate Statistics 4
B.2 Imputation of Age-Specific Migration Flows in 1980 4
B.3 Impacts of Depopulation and Aging by Variable 8
B.4 Impacts of Depopulation and Aging: Regression Results and First Stages . . 9
B.5 Decomposition of Cross-Regional Variation of Newborn 11

C Calibration Details **12**
C.1 Imputation of Labor Compensation by Municipality-Age-Year 12
C.2 Calibration of Amenity and Migration Costs 12
C.3 Model Validation using Data from 1990-2015 13

D Appendix for Quantitative Analysis **15**

A Data Sources

Table A.1: Data Sources

Category	Variables	Spatial Unit	Statistics Name	Source
(A) Population	Population by Age, Gender, and Residence 5 Yeas Ago	Municipality	Population Census	Ministry of Internal Affairs
	Fertility Rates by Mothers' Age	Prefecture	Vital Statistics	Ministry of Health, Labour and Welfare
	Death Rates by Age and Gender	Prefecture	Vital Statistics	Ministry of Health, Labour and Welfare
	Projected Fertility and Mortality Rates	National		Institute of Population and Social Security Research
(B) Income / Employment	Taxable Income	Municipality	Tax Statistics	Ministry of Internal Affairs
	Number Of Workers by Sector	Municipality	Economic Census	Ministry of Internal Affairs
	Number Of Establishments by Sector	Municipality	Economic Census	Ministry of Internal Affairs
	Wage by Age, Gender, Sector, Occupation	Prefecture	Basic Survey on Wage Structure	Ministry of Health, Labour and Welfare
(C) Housing / Land	Total Number Of Residences	Municipality	Housing and Land Survey	Ministry of Internal Affairs
	Posted Land Price	Municipality	Posted Land Price Statistics	Ministry of Land, Infrastructure, Transport and Tourism
(D) Amenity				
Retail	Number Of Retail Stores	Municipality	Economic Census	Ministry of Internal Affairs
	Number Of Large Retail Stores	Municipality	Economic Census	Ministry of Internal Affairs
	Number of Clothing Stores	Municipality	Economic Census	Ministry of Internal Affairs
	Number of Food and Beverage Retail Stores	Municipality	Economic Census	Ministry of Internal Affairs
	Number Of Restaurants	Municipality	Economic Census	Ministry of Internal Affairs
	Number Of Barber Shops And Beauty Parlors	Municipality	Report on Public Health Administration and Services	Ministry of Health, Labour and Welfare
Public Service	Number Of Libraries	Municipality	Prefecture Statistics	Prefecture Office
	Number Of Post Office	Municipality	Post Office Statistics	Post Office
	Road Length	Municipality	Road Infrastructure Statistics	Ministry of Land, Infrastructure, Transport and Tourism
	Paved Road Length	Municipality	Road Infrastructure Statistics	Ministry of Land, Infrastructure, Transport and Tourism
	Number Of Parks	Municipality	Park Statistics	Ministry of Land, Infrastructure, Transport and Tourism
	Area Of Parks	Municipality	Park Statistics	Ministry of Land, Infrastructure, Transport and Tourism
	Number Of Police Stations	Municipality	Prefecture Statistics	Prefecture Office
Eldery Service	Number Of Nursing Homes	Municipality	Report on Public Health Administration and Services	Ministry of Health, Labour and Welfare
	Number Of Community Centers	Municipality	Social and Education Statistics	Ministry of Education, Culture, Sports, Science and Technology
	Number Of Senior Citizen Clubs	Municipality	Prefecture Statistics	Prefecture Office
Child/Education	Number Of Daycares	Municipality	Social and Wlfare Statistics	Ministry of Health, Labour and Welfare
	Number Of Schools (Elementary, Middle, and High)	Municipality	Prefecture Statistics	Prefecture Office
	Number Of Teachers (Elementary, Middle, and High)	Municipality	School Statistics	Ministry of Education, Culture, Sports, Science and Technology
Health/Medical	Number Of General Hospitals	Municipality	Survey of Medical Institutions	Ministry of Health, Labour and Welfare
	Number Of General Clinics	Municipality	Survey of Medical Institutions	Ministry of Health, Labour and Welfare
	Number Of Medical Doctors	Municipality	Statistics of Physicians, Dentists and Pharmacists	Ministry of Health, Labour and Welfare
	Number Of Nurses	Municipality	Prefecture Statistics	Prefecture Office

Note: Table A.1 summarizes the main data sources used in the paper, together with the corresponding variables, spatial units, statistical products, and source agencies. Unless otherwise noted, the data are harmonized to the 2015 municipality definition.

Table A.2: PCA Loading for Amenity Categories

	Loading
Panel A. Child/Education	
Number of Daycares	0.508
Number of Libraries	0.440
Number of Schools (Elementary, Middle, and High)	0.515
Number of Teachers (Elementary, Middle, and High)	0.533
Panel B. Elderly Service	
Number of Community Centers	0.540
Number of Nursing Homes	0.569
Number of Senior Citizen Clubs	0.620
Panel C. Enviro/Transport	
Number of Parks	0.420
Paved Road Length	0.554
Number of Police Stations	0.503
Road Length	0.514
Panel D. Health/Medical	
Number of General Clinics	0.500
Number of General Hospitals	0.485
Number of Medical Doctors	0.514
Number of Nurses	0.501
Panel E. Retail	
Number of Car Dealerships	0.372
Number of Barber Shops and Beauty Parlors	0.386
Number of Clothing Stores	0.382
Number of Food and Beverage Retail Stores	0.383
Number of Large Retail Stores	0.352
Number of Restaurants	0.381
Number of Retail Stores	0.389

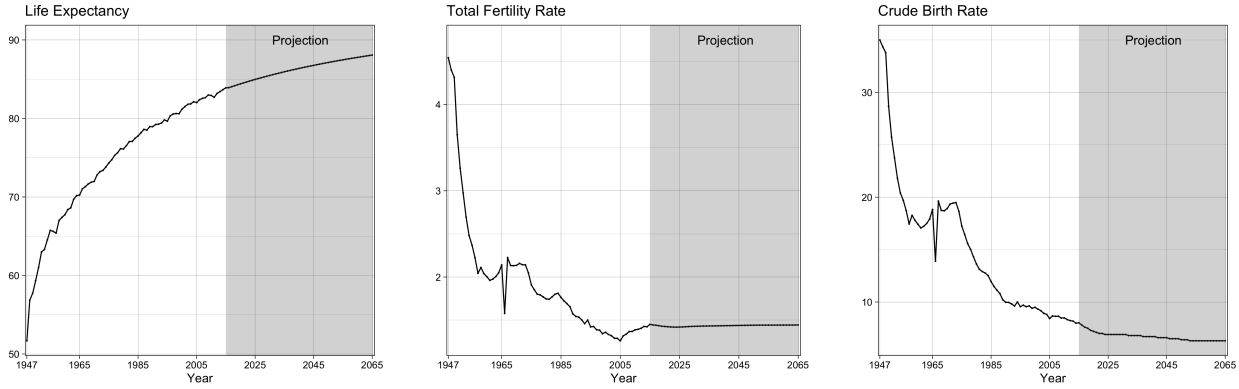
Note: Table A.2 reports the loading coefficients from the first principal component used to construct the amenity indices for each category. Higher loadings indicate that the corresponding variable contributes more strongly to the category-specific amenity index.

B Appendix for Reduced-Form Facts

This appendix provides additional evidence for the reduced-form analysis. We first report aggregate demographic statistics and additional descriptive evidence on the cross-municipality distribution of population density and aging, as well as the evolution of net migration rates across municipalities grouped by their elderly share in 1980. We then present the detailed IV results underlying the reduced-form estimates, including outcome-by-outcome coefficients, first-stage regressions, and a decomposition showing that regional variation in child population is largely accounted for by differences in the size and age composition of the reproductive population.

B.1 Aggregate Statistics

Figure B.1: Life Expectancy and Fertility Rates



Note: Figure B.1 plots life expectancy, the total fertility rate, and the crude birth rate in Japan. Historical data are shown through 2015, and projections from the National Institute of Population and Social Security Research are shown thereafter.

B.2 Imputation of Age-Specific Migration Flows in 1980

This appendix describes how we construct projected initial migration shares used in the IV strategy to proxy for age-specific bilateral migration patterns in 1980.

We estimate migration costs for each age group separately by implementing the Pseudo-Poisson Maximum Likelihood (PPML) estimator and using five-year bilateral migration flow data from the 2015 Census by age group.

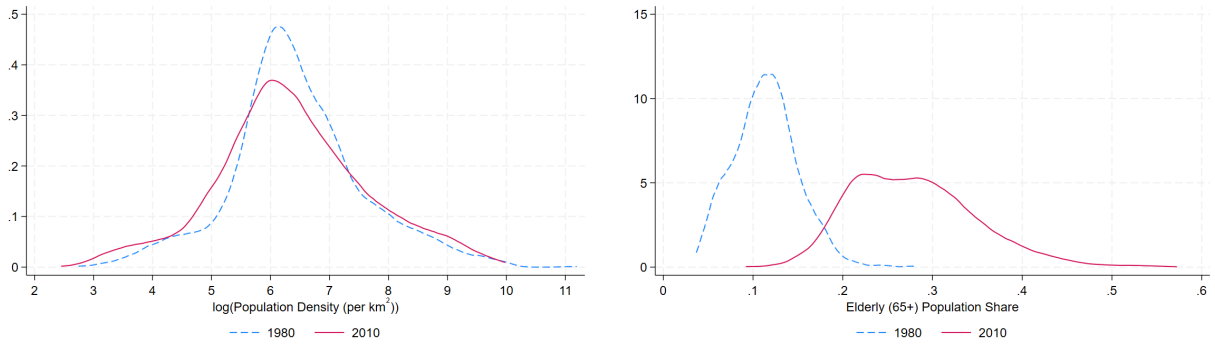
More precisely, we estimate the following equation which is consistent with the migration share equation (11):

$$\text{Migration}_{2015}^{ni}(a) = \exp\left(\boldsymbol{X}^{ni}\boldsymbol{\beta}(\boldsymbol{a}) + \text{Origin}_n(a) + \text{Destination}_i(a)\right) + \varepsilon_{ni}(a), \tag{B.1}$$

where $\text{Origin}_n(a)$ and $\text{Destination}_i(a)$ are fixed effects for origin and destination locations. $\boldsymbol{X}^{ni}$ is a vector of bilateral variables including the log of bilateral distance and various dummy variables. These dummy variables include indicators for home ($n = i$), within-prefecture

Figure B.2: Heterogeneity of Depopulation and Aging across Municipalities in Japan

(a) Population Density (b) Fraction of Population above 65 Years Old



Note: Figure B.2 reports the distribution of municipal population density in 1980 and 2010 in Panel (A) and the distribution of the municipal elderly share in the same years in Panel (B).

migration, within-area migration, within-island migration, east-west border migration, and adjacency of prefectures (see Wrona (2018) for the definition of the area, island, and border dummy variables). We also include interaction terms that involve the within-prefecture dummy variable with log of distance and with log of the area of the prefecture, respectively. We use the estimated results of this equation to recover the migration costs $(-\hat{\tau}^{ni}(a)/\nu = \boldsymbol{X}^{ni}\hat{\boldsymbol{\beta}}(\boldsymbol{a}))$.

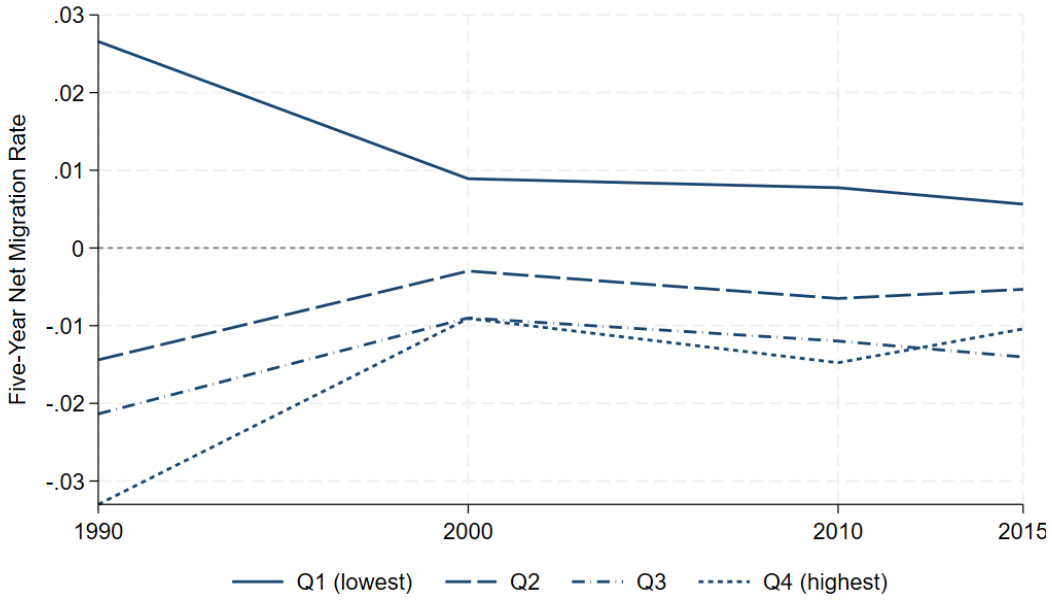
We normalize the cost of staying in the same location to zero, $\tau^{nn}(a) = 0$, and approximate bilateral migration flows using the implied gravity structure. To recover continuation values, we combine these estimated migration costs with observed population distributions in consecutive periods. In particular, we use municipality-level population data by age group in 1980 and 1985, together with the demographic accounting equation (13) and the migration share equation (11), to obtain:

$$L^i_{t+1}(a) = \sum_n \left(\frac{\exp\left[s^n_t(a)\beta V^i_{t+1}(a+1) - \tau^{ni}_t(a)\right]^{1/\nu}}{\sum_\ell \exp\left[s^n_t(a)\beta V^\ell_{t+1}(a+1) - \tau^{n\ell}(a)\right]^{1/\nu}} s^n_t(a-1) L^n_t(a-1) \right). \tag{B.2}$$

Given observed population distributions $\{L^n_t(a)\}$ and $\{L^n_{t+1}(a)\}$, survival rates $\{s^n_t(a)\}$, structural parameters β and ν, and migration costs $\{\tau^{ni}_t(a)\}$, we can uniquely recover the continuation values $\{V^i_{t+1}(a+1)\}$ up to a normalization.[1] Using these recovered continuation values, we compute bilateral migration flows implied by the model.

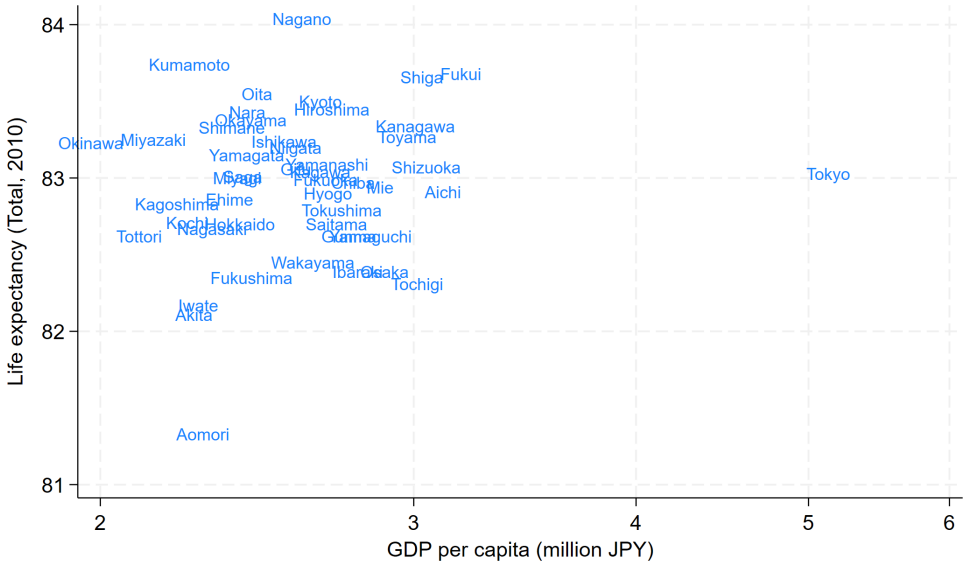
[1] As shown in Allen and Arkolakis (2014) and Redding and Rossi-Hansberg (2017) in static settings, this inversion identifies continuation values up to scale, as one equation is redundant.

Figure B.3: Net In-Migration Rates by Initial Elderly Share



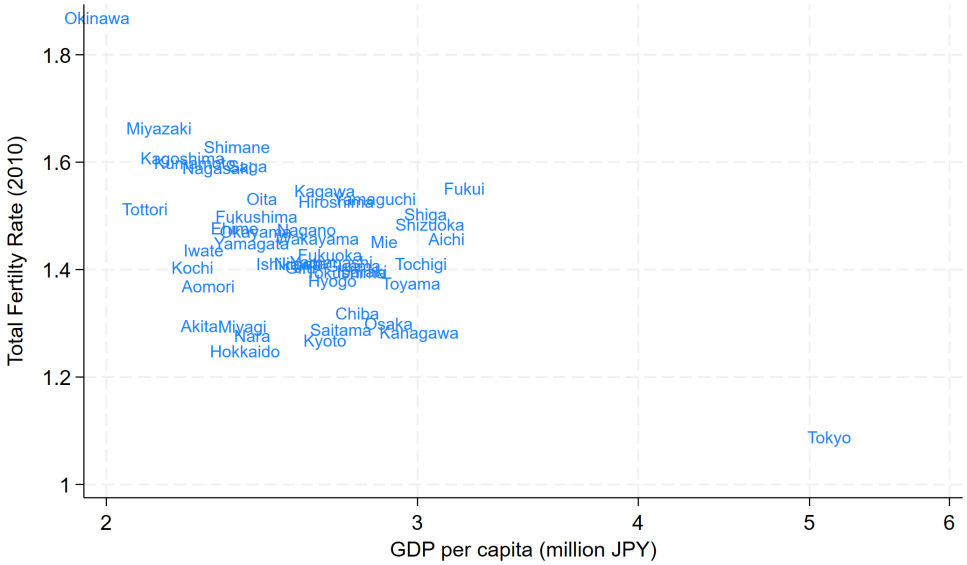
Note: Figure B.3 reports net in-migration rates in 1990, 2000, 2010, and 2015. Each line reports the average outcome for municipalities grouped into quartiles based on their initial share of the elderly population (aged 65 or above) in 1980, with Q1 representing the lowest share and Q4 the highest. Net in-migration in year t is defined as inflows between $t-5$ and t minus outflows over the same period. The net in-migration rate divides this value by population in year $t-5$. Migration data are obtained from the Population Census and are based on bilateral migration flows between municipalities. The data are available for 1990, 2000, and 2010, and for every census thereafter. To ensure consistency over time, municipalities are harmonized to the 2015 municipality definition. For municipalities affected by mergers, bilateral migration flows are aggregated across constituent municipalities before calculating migration measures. To the best of our knowledge, age-specific bilateral migration data at the municipality level are publicly available only from the 2015 Census onward.

Figure B.4: Cross-Prefectural Variation in Life Expectancy in 2010



Note: Figure B.4 plots life expectancy against prefectural income per capita in 2010. Life expectancy is obtained from the National Institute of Population and Social Security Research, and prefectural income per capita is from the Prefectural Accounts.

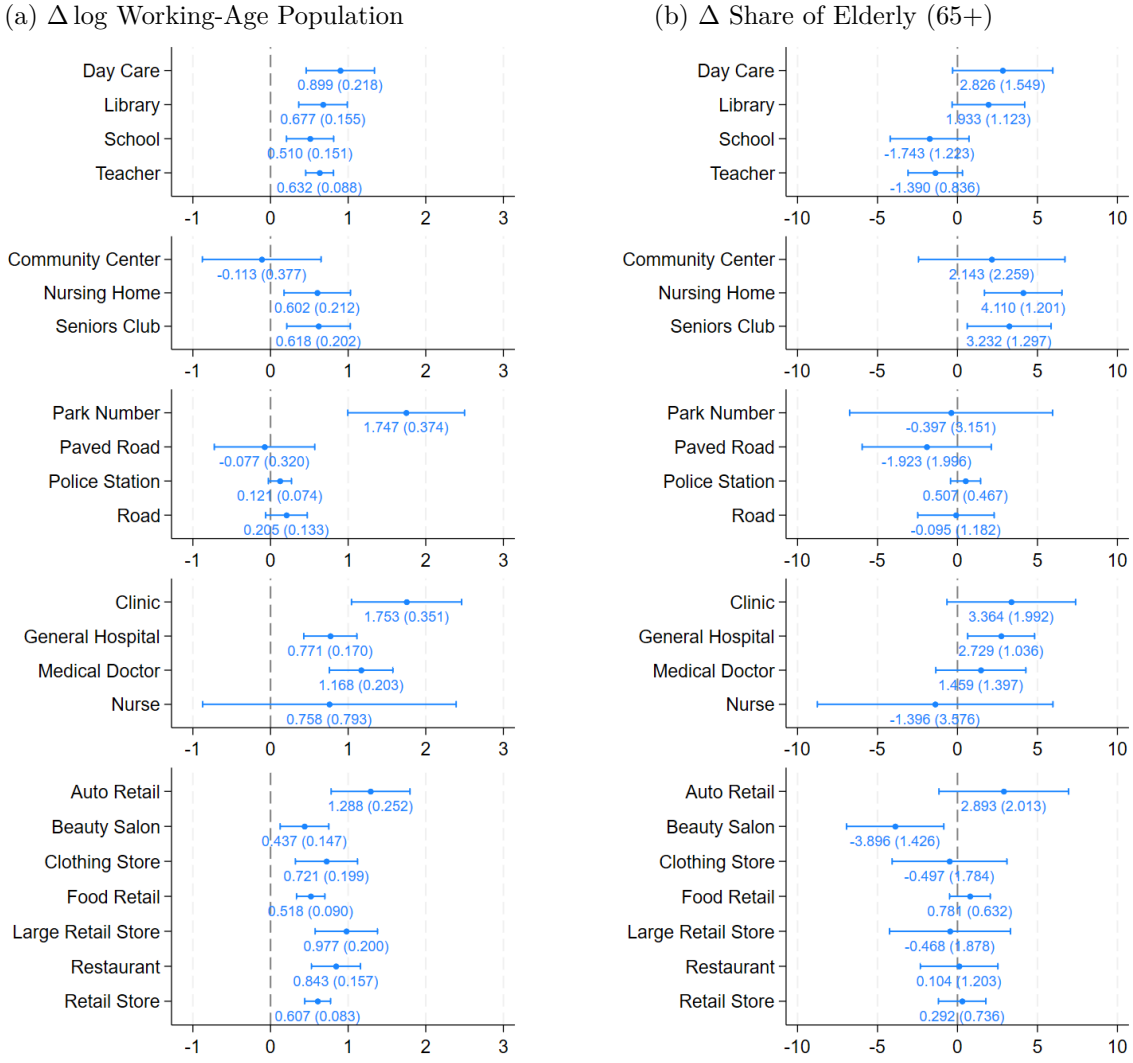
Figure B.5: Cross-Prefectural Variation in TFR in 2010



Note: Figure B.4 plots the total fertility rate (TFR) against prefectural income per capita in 2010. The TFR is constructed using births from the Vital Statistics and population data from the Census, while prefectural income per capita is from the Prefectural Accounts.

B.3 Impacts of Depopulation and Aging by Variable

Figure B.6: Impacts of Depopulation and Aging on Local Economy by Variable



Note: Figure B.6 reports the coefficient estimates from equation (4) for the individual amenity variables underlying the PCA indices. The left panel reports the coefficients on Δ log working-age population, and the right panel reports the coefficients on Δ share of the elderly. Horizontal bars indicate 95% confidence intervals for the reported estimates.

B.4 Impacts of Depopulation and Aging: Regression Results and First Stages

Table B.1: Impacts of Depopulation and Aging on Local Economy

VARIABLES	(1) Child/ Education	(2) Elderly Service	(3) Env./ Transport	(4) Health/ Medical	(5) Retail	(6) Local Gov. Spending (pc)	(7) Personal Inc. Tax (pc)	(8) Residence	(9) Housing Construction	(10) Land Price (Housing)
Δ log Working-Age Population	0.597***	0.498***	0.169***	0.690***	0.652***	-0.532***	0.00221	0.898***	0.926**	1.023***
	(0.106)	(0.178)	(0.0388)	(0.172)	(0.106)	(0.110)	(0.0705)	(0.175)	(0.436)	(0.230)
Δ Share of Elderly Population	0.652	2.538**	0.938***	-1.003	-2.931*	0.248	-0.801**	-1.640	6.438	4.235*
	(0.958)	(1.235)	(0.290)	(1.471)	(1.566)	(0.900)	(0.349)	(2.321)	(3.838)	(2.427)
Observations	965	933	1333	736	602	1729	1729	645	643	863
Controls	Yes	Yes	Yes	Yes	Yes	Yes	Yes	Yes	Yes	Yes
Prefecture FE	Yes	Yes	Yes	Yes	Yes	Yes	Yes	Yes	Yes	Yes
Kleibergen-Paap F	15.13	9.615	15.83	15.00	18.53	43.32	43.32	23.00	9.144	16.40

Note: Table B.1 reports the coefficient estimates for the local-economy outcomes discussed in Section 3.2. Controls include employment shares in the secondary and tertiary sectors, total land area (in logs), total population density (in logs), the ratio of habitable land area to total land area (in logs), the share of elderly, the share of children (under age 15), and the skilled-to-unskilled ratio (in logs, where skilled workers are defined as college graduates or above), all measured in 1980, as well as taxable income per capita (in logs) in 1985. Robust standard errors are clustered at the prefecture level and reported in parentheses. The ***, **, and * represent statistical significance at the 0.01, 0.05, and 0.10 levels, respectively.

Table B.2: First-Stage Regressions for Demographic Changes

VARIABLES	(1) Δ log Working-Age Population	(2) Δ Share of Elderly Population
Pull IV (Working-Age	-0.342**	0.0717***
Population)	(0.129)	(0.0138)
Pull IV (Elderly Population)	-0.368***	0.0789***
	(0.108)	(0.0102)
Push IV (Working-Age	1.274***	-0.236***
Population)	(0.197)	(0.0240)
Push IV (Elderly Population)	-0.258**	0.136***
	(0.101)	(0.0159)
Observations	1,729	1,729
Controls	Yes	Yes
Prefecture FE	Yes	Yes
Excluded IV F-statistic	27.70	38.35

Note: Table B.2 reports the first-stage regressions for the demographic-change measures used in the reduced-form analysis. Controls include employment shares in the secondary and tertiary sectors, total land area (in logs), total population density (in logs), the ratio of habitable land area to total land area (in logs), the share of elderly, the share of children (under age 15), and the skilled-to-unskilled ratio (in logs, where skilled workers are defined as college graduates or above), all measured in 1980, as well as taxable income per capita (in logs) in 1985. Robust standard errors are clustered at the prefecture level and reported in parentheses. The ***, **, and * represent statistical significance at the 0.01, 0.05, and 0.10 levels, respectively.

B.5 Decomposition of Cross-Regional Variation of Newborn

To assess whether imposing a common national fertility schedule is a reasonable simplification, we construct the predicted number of children aged 0 to 4 in each location using the local reproductive-age population and national age-specific fertility rates:

$$\widehat{L}_t^n(0) = \sum_{a \in A} \varkappa_t(a) L_t^n(a). \tag{B.3}$$

The predicted number differs from the observed number of children because of regional fertility differences, mortality, migration, gender composition, and idiosyncratic variation. Denoting these factors by ε_t^n, we write

$$\ln L_t^{n,\text{obs}}(0) = \ln \widehat{L}_t^n(0) + \varepsilon_t^n. \tag{B.4}$$

Thus, the cross-regional variation in the child population satisfies

$$\text{Var}\left(\ln L_t^{n,\text{obs}}(0)\right) = \text{Var}\left(\ln \widehat{L}_t^n(0)\right) + \text{Var}\left(\varepsilon_t^n\right) + 2\text{Cov}\left(\ln \widehat{L}_t^n(0), \varepsilon_t^n\right). \tag{B.5}$$

We use this decomposition to assess how much of the cross-regional variation in child population can be accounted for by differences in reproductive-age population alone.

To quantify the contribution of each component, we divide both sides by $\text{Var}\left(\ln L_t^{n,\text{obs}}(0)\right)$:

$$1 = \underbrace{\frac{\text{Var}\left(\ln \widehat{L}_t^n(0)\right)}{\text{Var}\left(\ln L_t^{n,\text{obs}}(0)\right)}}_{\simeq 1.06} + \underbrace{\frac{\text{Var}\left(\varepsilon_t^n\right)}{\text{Var}\left(\ln L_t^{n,\text{obs}}(0)\right)}}_{\simeq 0.01} + \underbrace{2\frac{\text{Cov}\left(\ln \widehat{L}_t^n(0), \varepsilon_t^n\right)}{\text{Var}\left(\ln L_t^{n,\text{obs}}(0)\right)}}_{\simeq -0.07}, \tag{B.6}$$

where the numbers below each term report the average value across years from 1980 to 2010.

The covariance term is negative, which is consistent with the fact that population is increasingly concentrated in high-density areas where fertility rates tend to be below the national average. In such areas, applying national fertility rates tends to overpredict the number of children relative to the observed level, generating a negative covariance between the predicted component and the residual. The first term, which captures the contribution of the predicted component under national fertility rates, ranges from 1.02 to 1.11 across years, peaks in 1995, and declines thereafter, reaching 1.02 in 2010. Differences in the distribution of reproductive-age population play a dominant role in shaping the spatial distribution of children, allowing us to abstract from regional fertility differences without substantially distorting the main patterns in the data.

C Calibration Details

This appendix section provides additional details on how the calibration is implemented in practice. We first explain how municipality-by-age labor compensation is imputed from prefecture-level wage and employment data together with municipal taxable income. We then describe the normalization and inversion procedure used to recover amenities and bilateral migration costs, report the reduced-form estimation of migration frictions, and validate the calibrated model by fixing exogenous fundamentals at their 1990 levels.

C.1 Imputation of Labor Compensation by Municipality-Age-Year

Due to the unavailability of labor income data by age group at the municipality level, we impute the municipality-level effective wage for age group a:

$$\varphi_t^n(a) = \bar{\varphi}_t^n \times w_t^{pref}(a) \times \text{Employment Rate}_t^{pref}(a), \tag{C.1}$$

where $\bar{\varphi}_t^n$ represents the TFP of municipality n, $w_t^{pref}(a)$ represents the wage for age group a within the prefecture of the municipality, and $\text{Employment Rate}_t^{pref}(a)$ is the employment rate for the age group within the prefecture. Our underlying assumption is that wage rates and employment rates change consistently in the same way over the life cycle across municipalities within the same prefecture. We calibrate $\bar{\varphi}_t^n$ to align the total effective wage bill of the municipality with the observed taxable income data ($\text{Taxable Income}_t^n = \sum_a \varphi_t^n(a)$). Applying this equation, we can calibrate the municipality-level TFP by year as follows:

$$\bar{\varphi}_t^n = (\text{Taxable Income}_t^n)/(\sum_a w_t^{pref}(a) \times \text{Employment Rate}_t^{pref}(a)) \tag{C.2}$$

By construction, there is no variation in productivity within the same prefecture and age group apart from the TFP. Therefore, we focus our estimates on productivity spillovers on TFP.

C.2 Calibration of Amenity and Migration Costs

We start by introducing three sets of normalization of these variables. First, we normalize the exogenous amenity $\tilde{\chi}_t^n(a)$ to one for all n, t, a, since exogenous amenity is isomorphic to in-migration costs in the previous period ($\tau_{t-1}^{in}(a-1)$ for all i) under our additive utility specification. Second, we normalize migration costs within a region such that $\tau_t^{nn}(a) = 0$ for all t, since the in-migration cost is isomorphic to out-migration costs in the subsequent period ($\tau_{t+1}^{ni}(a+1)$ for all i). Third, we normalize the housing sector productivity parameter $\widetilde{\xi}^n$ to one, as this term is absorbed into the amenity value. Note that these normalizations do not affect our equilibrium allocation and welfare implications; hence this is without loss of generality.

We then assume that bilateral migration frictions do not change after 2015. We back out off-diagonal elements of migration frictions, $\{\tau^{ni}(a)\}$, to precisely replicate the observed migration flows in 2015, $\{\mu_{2015}^{ni}(a)\}$. This is done recursively as follows. Assuming that the

functional form of and spillover elasticities on productivity and amenity as well as the other structural parameters and fundamentals are known, we carry out the following procedure:

1. Guess the set of value functions $\{V^n_{T+1}(a+1)\}_n$, where $T = 2015$.

2. Using the observed migration flow data at T, we first calibrate $\{\tau^{in}(a)\}$ using the following equation derived from equation (11):

$$\frac{\mu^{in}_T(a)}{\mu^{ii}_T(a)} = \exp\left[s^n_T(a)\beta V^n_{T+1}(a+1) - s^i_T(a)\beta V^i_{T+1}(a+1) - \tau^{in}(a)\right]^{1/\nu}, \tag{C.3}$$

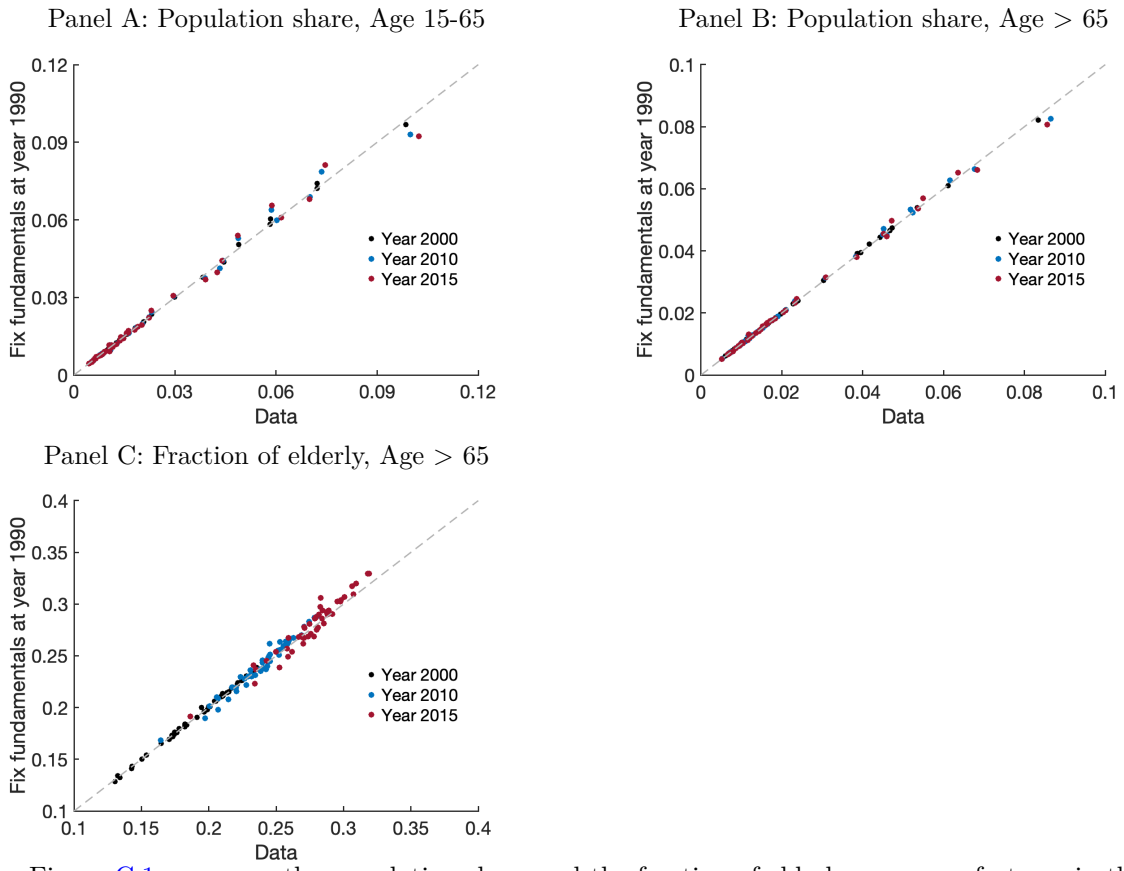
3. Given the parameters, functional forms, and the assumption that $\tau^{in}_t(a) = \tau^{in}(a)$ for all $t \geq T$, we can simulate the model forward starting at $t = T$ all the way toward $t = \infty$ and update the guess of the set of value functions $\{V^{n,implied}_{T+1}(a+1)\}_n$.

4. Iterate the steps from 1 to 3 until we find a fixed point in $\{V^{n,implied}_{T+1}(a+1)\}_n \to \{V^n_{T+1}(a+1)\}_n$.

C.3 Model Validation using Data from 1990-2015

To validate our model, we follow the same procedure of model calibration as described in Section 5.2, except that we instead set the initial period at 1990 (instead of 2015). We assume that fundamentals have been unchanged since 1990. Figure C.1 shows that our simulation predicts approximately the same patterns of population shares across prefectures as observed in the data in 2000, 2010, and 2015.

Figure C.1: Population Allocation: Set Initial Year to 1990, and Validate Population up to 2015

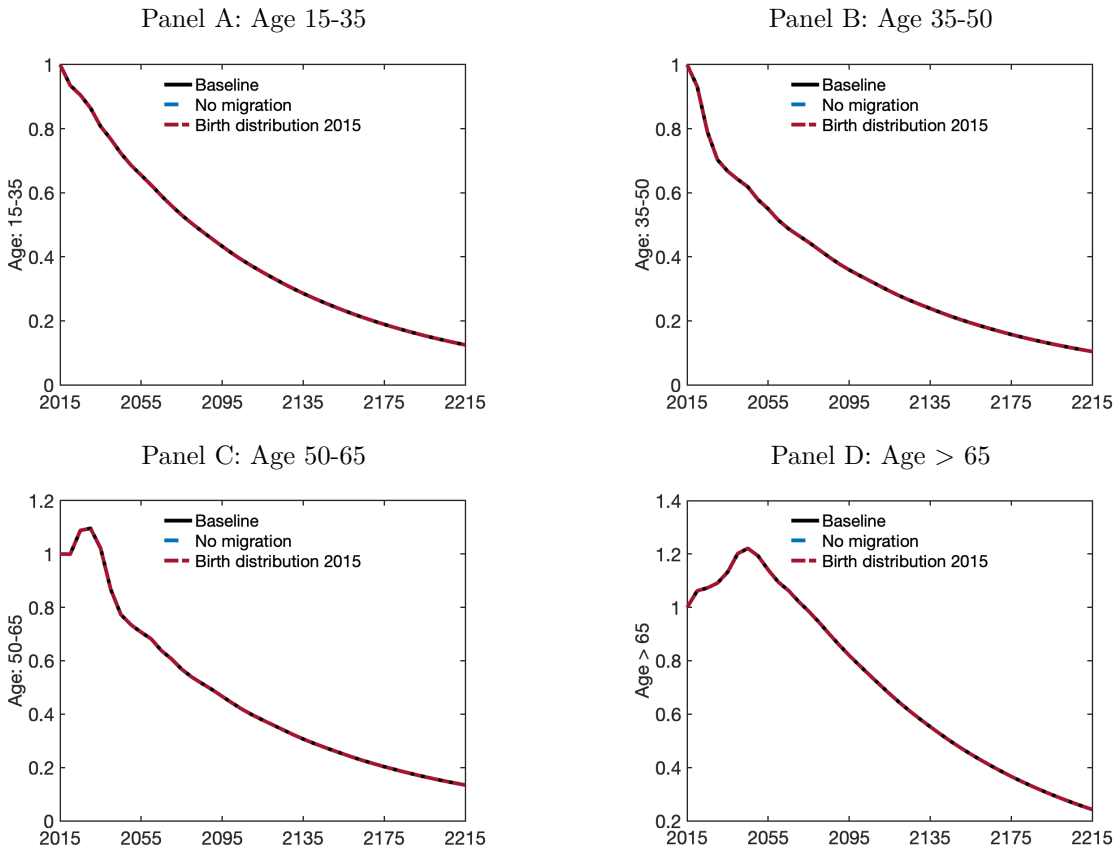


Note: Figure C.1 compares the population share and the fraction of elderly across prefectures in the data with those in a counterfactual scenario where exogenous fundamentals are fixed at their 1990 levels. Each observation is a prefecture.

D Appendix for Quantitative Analysis

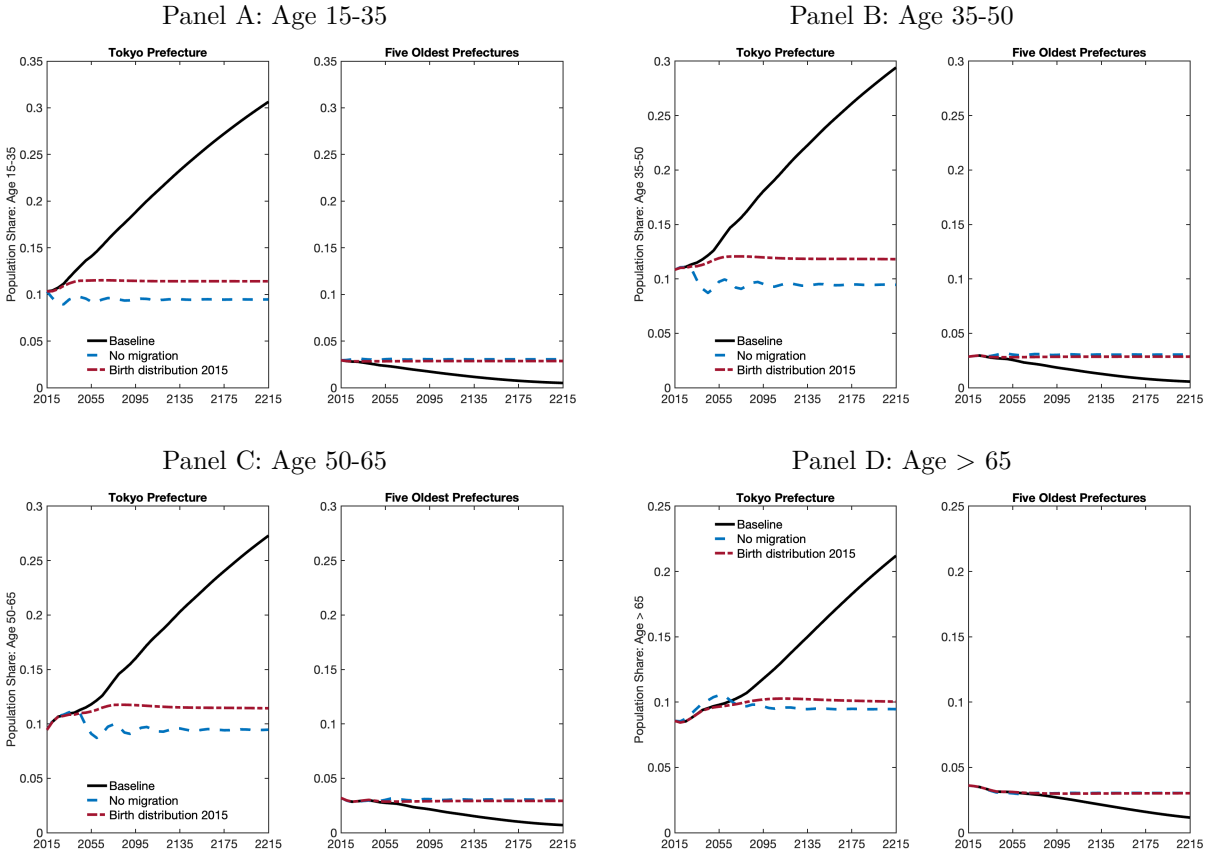
This appendix collects additional figures for the quantitative analysis. We first report the projected evolution of aggregate population and regional population shares separately by age group. We then provide supplementary figures on regional wages, housing rents, and flow utility, as well as the implied labor income tax rate. Finally, we report additional policy results that show how the effects of place-based transfers vary with policy duration.

Figure D.1: Population Size By Age Groups all over Japan



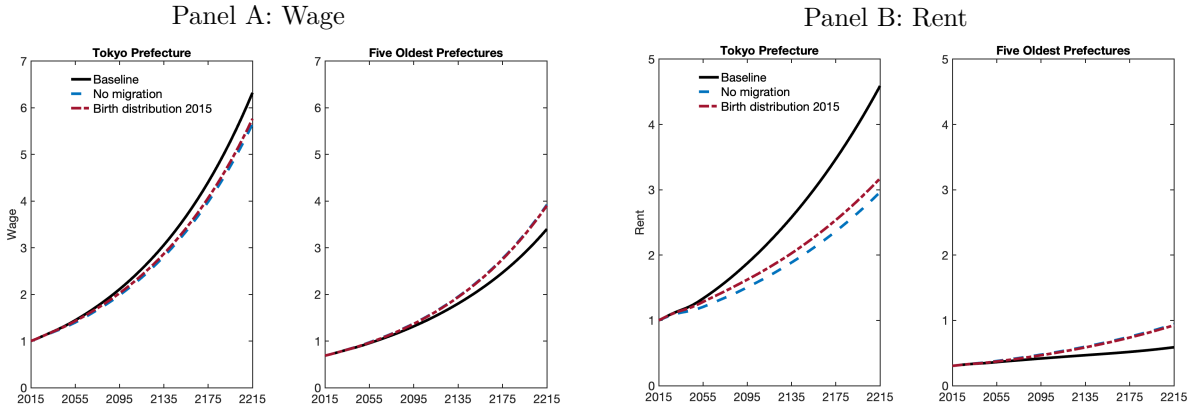
Note: Figure D.1 reports model-implied aggregate population paths for the four age groups shown in the panels under the baseline, no-migration, and birth-distribution-in-2015 specifications. Each series is normalized to one in 2015. Because migration only reallocates population across regions, the three specifications imply the same aggregate age-group paths.

Figure D.2: Population Share By Age Groups and Region



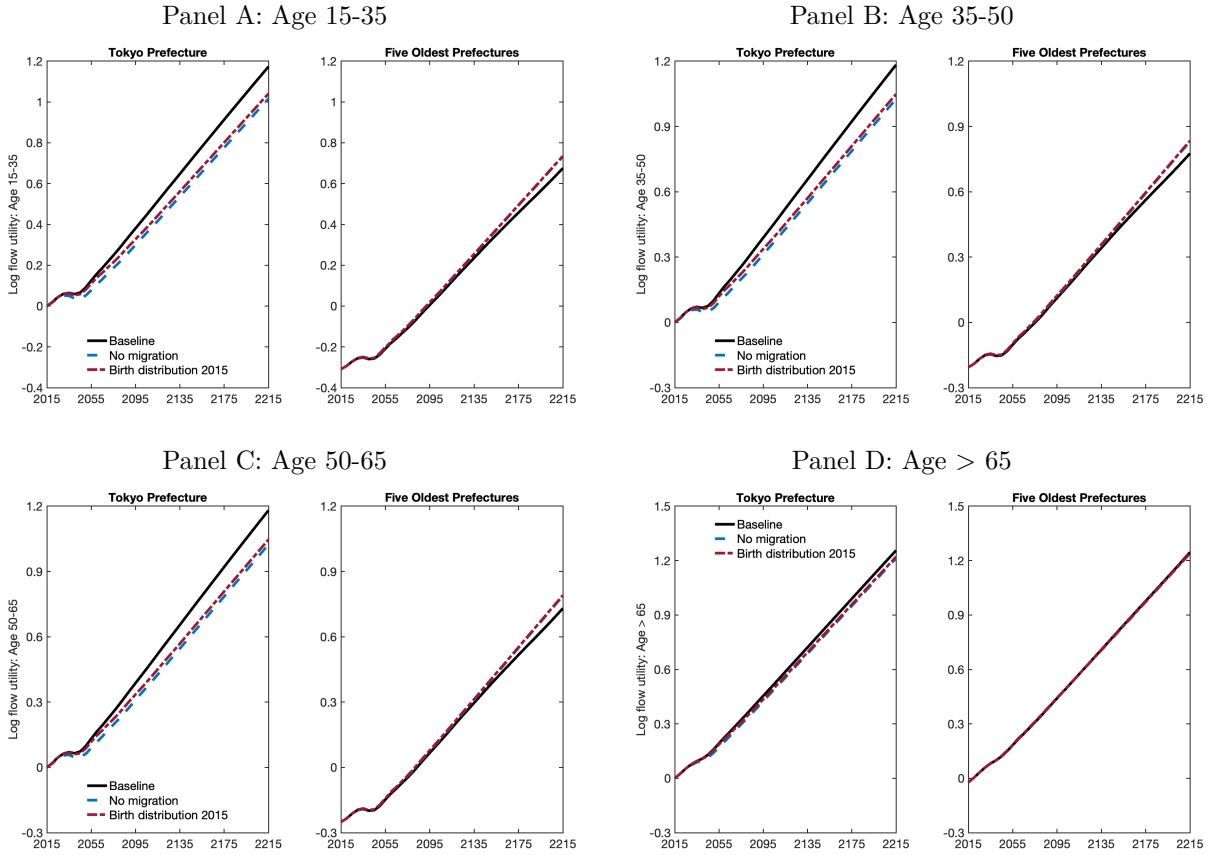
Note: Figure D.2 reports model-implied population shares for Tokyo prefecture and the five oldest prefectures as of 2015 under the baseline, no-migration, and birth-distribution-in-2015 specifications, separately for the four age groups shown in the panels.

Figure D.3: Wage and Housing Rent By Region



Note: Figure D.3 reports model-implied wages and housing rents for Tokyo prefecture and the five oldest prefectures as of 2015 under the baseline, no-migration, and birth-distribution-in-2015 specifications. Panel (A) shows wages, and Panel (B) shows housing rents.

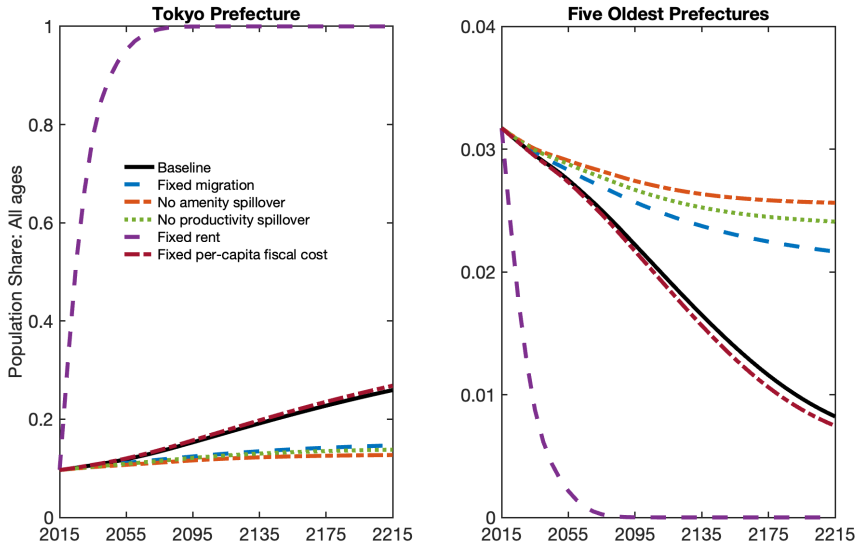
Figure D.4: Flow Utility



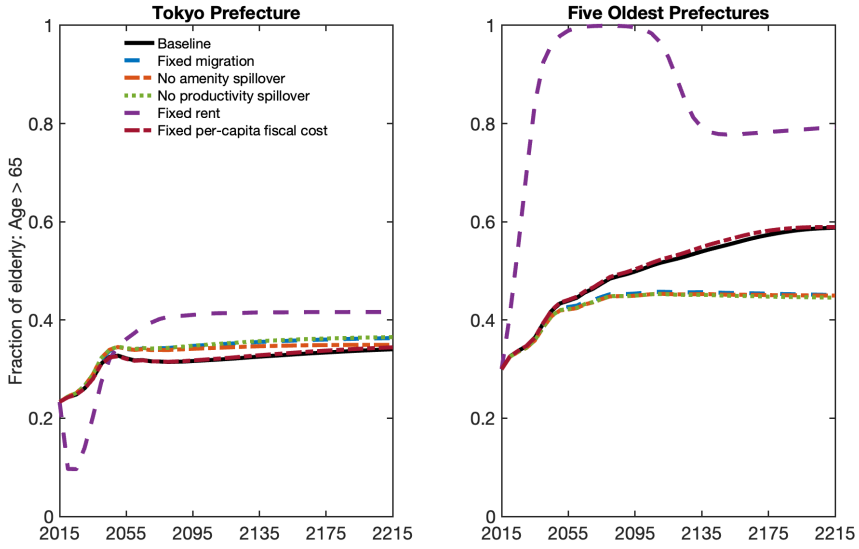
Note: Figure D.4 reports model-implied flow utility for Tokyo prefecture and the five oldest prefectures as of 2015 under the baseline, no-migration, and birth-distribution-in-2015 specifications, separately for the four age groups shown in the panels. Within each panel, values are normalized so that Tokyo in 2015 equals zero for the corresponding age group.

Figure D.5: Projected Population Shares across Locations, Shutting Down Different Channels

(A) Population Share



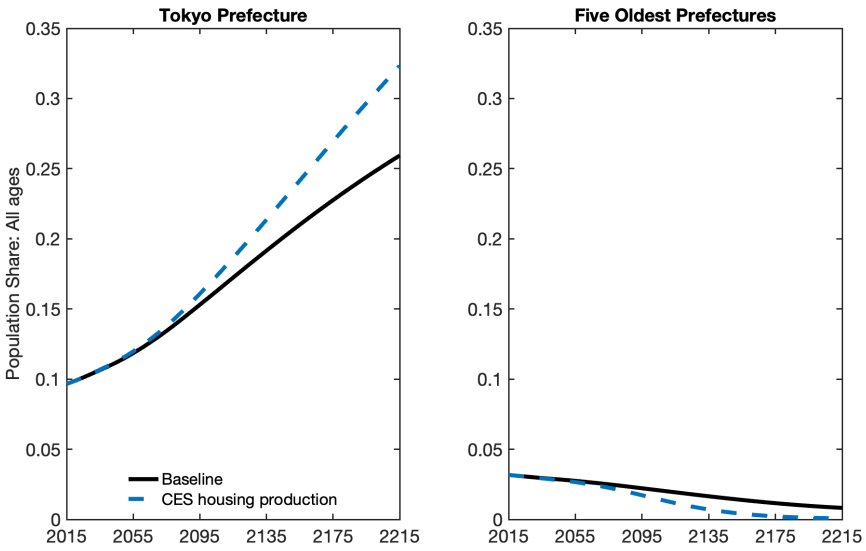
(B) Elderly Population Share



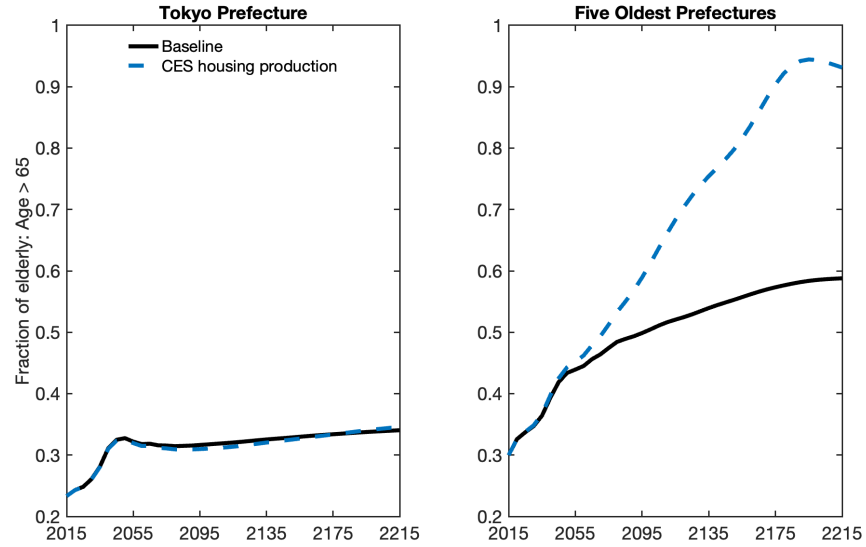
Note: Figure D.5 reports model-implied population shares for Tokyo prefecture and the five oldest prefectures as of 2015 under the baseline, fixed migration, no amenity spillover, no productivity spillover, fixed rent and fixed per-capita fiscal cost. Panel (A) shows total population shares, and Panel (B) shows elderly population shares.

Figure D.6: Projected Population Shares across Locations, CES Housing Production

(A) Population Share

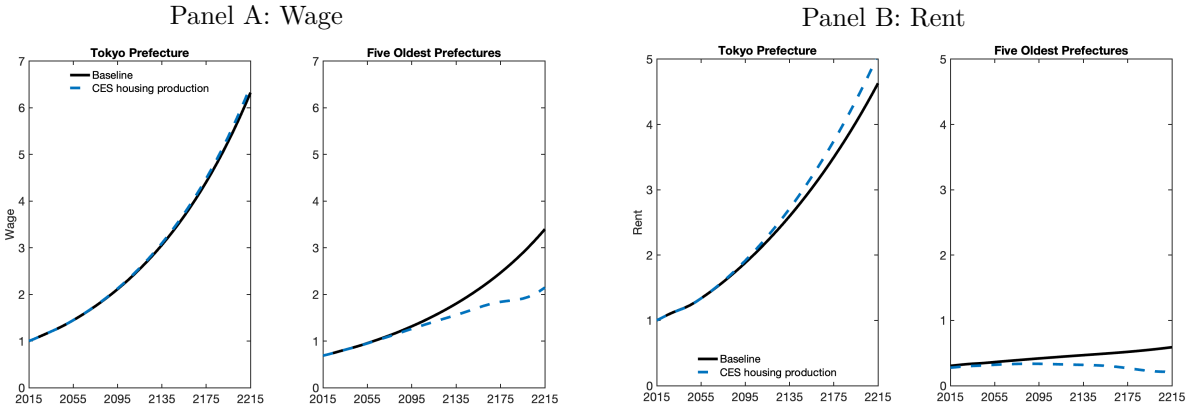


(B) Elderly Population Share



Note: Figure D.6 reports model-implied population shares for Tokyo prefecture and the five oldest prefectures as of 2015 under the baseline and CES housing specifications. Panel (A) shows total population shares, and Panel (B) shows elderly population shares. Appendix Figure D.2 presents the corresponding regional population-share paths separately by age group.

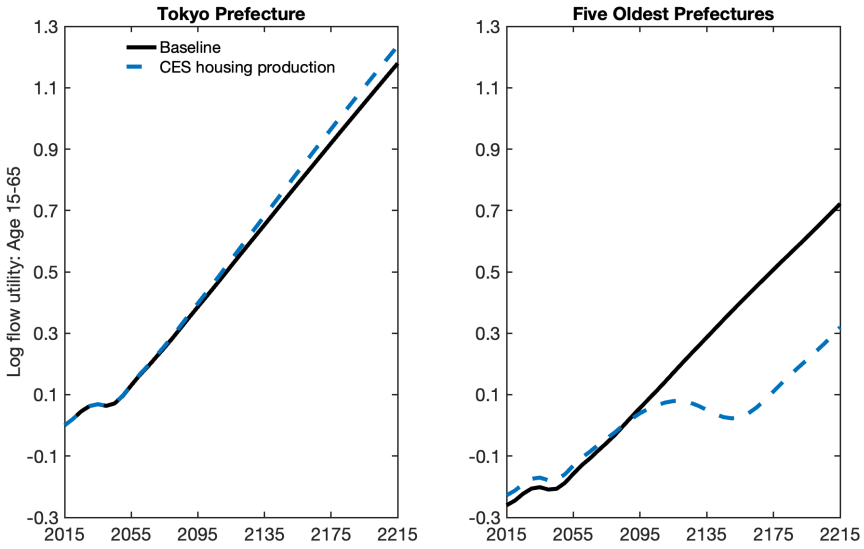
Figure D.7: Wage and Housing Rent By Region, CES Housing Production



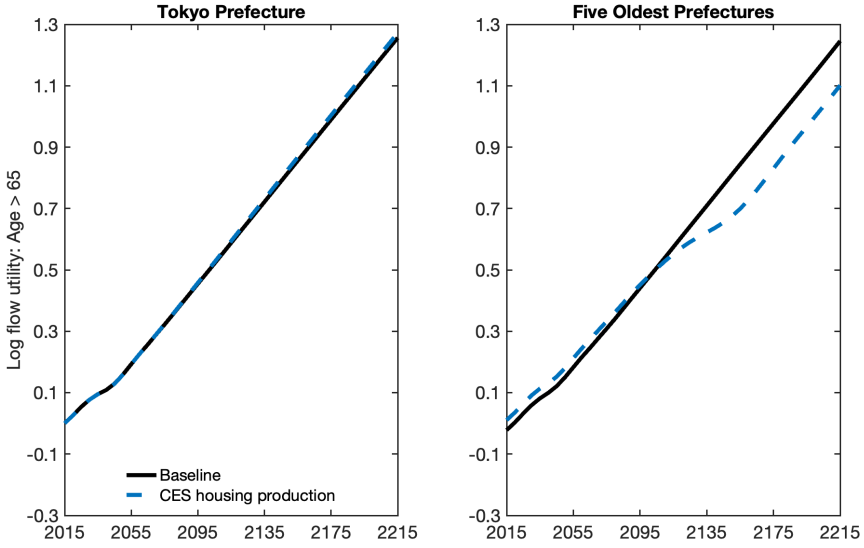
Note: Figure D.7 reports model-implied wages and housing rents for Tokyo prefecture and the five oldest prefectures as of 2015 under the baseline and CES housing specifications. Panel (A) shows wages, and Panel (B) shows housing rents.

Figure D.8: Flow Utility By Location, CES Housing Production

(A) Working-Age (Age 15-65)



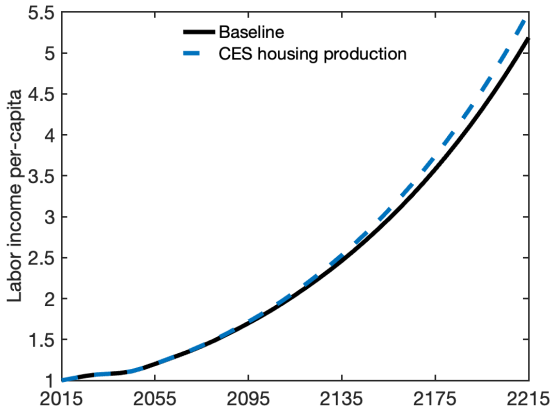
(B) Elderly (Over 65)



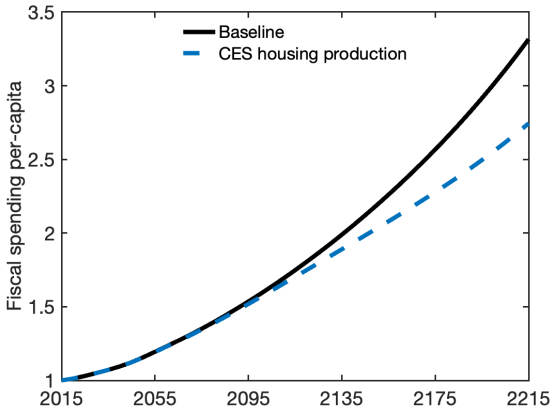
Note: Figure D.8 reports model-implied flow utility for Tokyo prefecture and the five oldest prefectures as of 2015 under the baseline and CES housing specifications. In each panel, values are normalized so that Tokyo in 2015 equals zero for the corresponding age group.

Figure D.9: Projected Aggregate Income and Fiscal Spending per Capita, CES Housing Production

(A) Aggregate Income per Capita

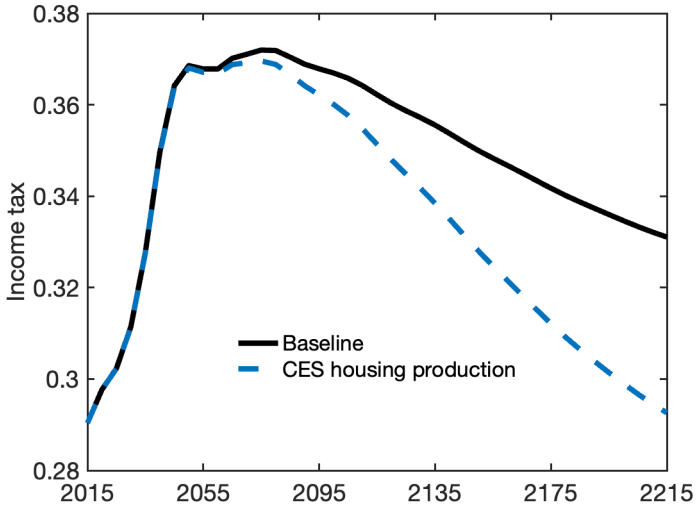


(B) Fiscal Spending per Capita



Note: Figure D.9 reports model-implied aggregate labor income per capita and fiscal spending per capita under the baseline and CES housing specifications. Each series is normalized to one in 2015.

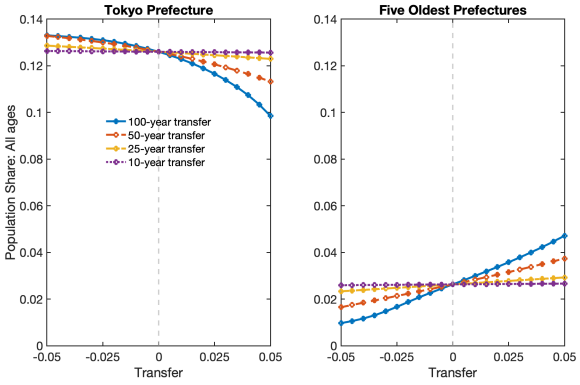
Figure D.10: Projected Labor Income Tax Rate, CES Housing Production



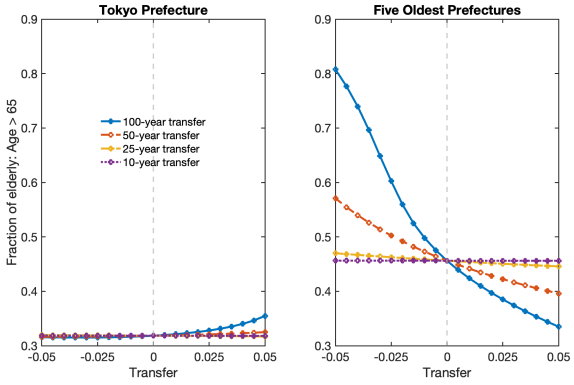
Note: Figure D.10 reports the model-implied labor income tax rate κ_t from 2015 onward under the baseline and CES housing specifications. The tax rate finances pensions and local public services in the model economy.

Figure D.11: Place-based Transfers with Alternative Durations

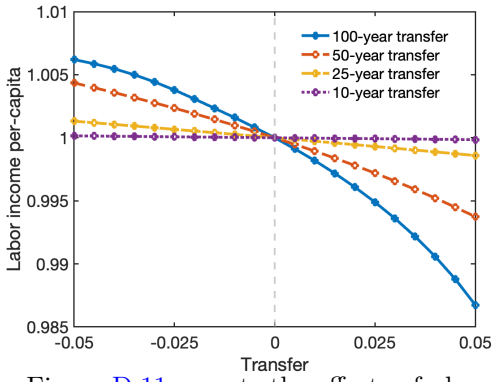
Panel A: Population Share



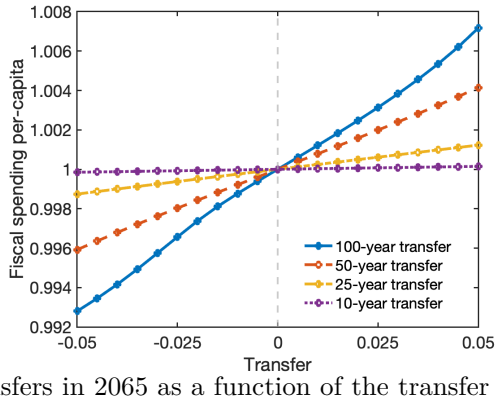
Panel B: Fraction of elderly



Panel C: Aggregate Income per Capita



Panel D: Fiscal Spending per Capita



Note: Figure D.11 reports the effects of place-based transfers in 2065 as a function of the transfer rate to the five oldest prefectures relative to their labor and pension income combined, financed by a proportional labor-income tax on Tokyo residents. Panel (A) shows population shares, Panel (B) shows the fraction of elderly, Panel (C) shows aggregate labor income per capita, and Panel (D) shows fiscal spending per capita. Different lines correspond to different policy durations.